

1 **Double-negative T cells have a reparative role after experimental severe**  
2 **ischemic acute kidney injury**

3

4 Kyungho Lee,<sup>1,3</sup> Sepideh Gharaie,<sup>1</sup> Johanna T. Kurzhagen,<sup>1</sup> Andrea M. Newman-Rivera,<sup>1</sup> Lois J.  
5 Arend,<sup>2</sup> Sanjeev Noel<sup>1</sup> & Hamid Rabb<sup>1</sup>

6

7 <sup>1</sup>Department of Medicine, <sup>2</sup>Department of Pathology, Johns Hopkins University School of  
8 Medicine, Baltimore, Maryland

9 <sup>3</sup>Nephrology Division, Department of Medicine, Samsung Medical Center, Cell and Gene  
10 Therapy Institute, Sungkyunkwan University School of Medicine, Seoul, Korea

11

12 **RUNNING HEAD:** Role of double-negative T cells in AKI-repair

13

14 Correspondence

15 Hamid Rabb, M.D.

16 The Johns Hopkins Hospital

17 720 Rutland Avenue, Ross 965

18 Baltimore, MD, USA 21205

19 Email: [hrabb1@jhmi.edu](mailto:hrabb1@jhmi.edu)

20 **ABSTRACT**

21 T cells mediate organ injury and repair. A proportion of unconventional kidney T cells called  
22 double-negative (DN) T cells ( $\text{TCR}^+ \text{CD4}^- \text{CD8}^-$ ), with anti-inflammatory properties, were  
23 previously demonstrated to protect from early injury in moderate experimental AKI. However,  
24 their role in repair after AKI has not been studied. We hypothesized that DN T cells mediate  
25 repair after severe AKI. C57B6 mice underwent severe (40min) unilateral ischemia-reperfusion  
26 injury (IRI). Kidney DN T cells were studied by flow cytometry and compared to gold-standard  
27 anti-inflammatory  $\text{CD4}^+$  Tregs. In vitro effects of DN T cells and Tregs on renal tubular  
28 epithelial cell (RTEC) repair after injury were quantified with live-cell analysis. DN T cells,  
29 Tregs, CD4 or vehicle were adoptively transferred after severe AKI. Glomerular filtration rate  
30 (GFR) was measured using FITC-sinistrin. Fibrosis was assessed with Masson's trichrome  
31 staining. Profibrotic genes were measured with qRT-PCR. Percentages and the numbers of DN T  
32 cells substantially decreased during repair phase after severe AKI, as well as their activation and  
33 proliferation. Both DN T cells and Tregs accelerated RTEC cell repair in vitro. Post-AKI transfer  
34 of DN T cells reduced kidney fibrosis and improved GFR, as did Treg transfer. DN T cell  
35 transfer lowered  $\text{TGF}\beta 1$  and  $\alpha\text{SMA}$  expression. DN T cells reduced effector-memory  $\text{CD4}^+$  T  
36 cells and IL-17 expression. DN T cells undergo quantitative and phenotypical changes after  
37 severe AKI, accelerate RTEC repair in vitro as well as improve GFR and renal fibrosis in vivo.  
38 DN T cells have potential as immunotherapy to accelerate repair after AKI.

39

40 **NEW & NOTEWORTHY**

41 Double-negative (DN) T cells (CD4<sup>-</sup> CD8<sup>-</sup>) are unconventional kidney T cells with regulatory  
42 abilities. Their role in repair from AKI is unknown. Kidney DN T cell population decreased  
43 during repair after ischemic AKI, in contrast to Tregs which increased. DN T cell administration  
44 accelerated tubular repair in vitro, while after severe in vivo ischemic injury reduced kidney  
45 fibrosis and increased GFR. DN T cell infusion is a potential therapeutic agent to improve  
46 outcome from severe AKI.

47

48 **Keywords:** Acute kidney injury; ischemia-reperfusion injury; lymphocytes; repair; T cells

49

## 50 INTRODUCTION

51 Acute kidney injury (AKI) is a common and serious clinical problem resulting in high morbidity  
52 and mortality world-wide (1). Impaired recovery from AKI can lead to kidney fibrosis and  
53 transition to chronic kidney disease (CKD) (2). Although prior studies mostly focused on the  
54 prevention of early injury (3), understanding molecular and cellular mechanisms of repair and  
55 recovery after AKI is clinically important given that most patients are diagnosed after AKI has  
56 occurred (4).

57 Among the many cellular and molecular pathways involved in the AKI repair process (3, 5-9),  
58 immune responses mediated by T cells have been proposed as one of the important pathways (10,  
59 11). Long-term increase in numbers, immuno-phenotypical changes and transcriptomic  
60 reprogramming of T cells have been demonstrated in previous studies (12-14), highlighting their  
61 potential role in AKI repair or CKD transition. Furthermore, a minor proportion of kidney CD4<sup>+</sup>  
62 T cells, regulatory T cells (Tregs) that have anti-inflammatory properties not only have a  
63 protective role in early injury (15), but also have a reparative role in AKI to CKD transition (16).

64 An unconventional T cell subset, double-negative (DN) T cells that do not express either CD4  
65 nor CD8 exist in kidneys (17-20). While they are rarely present in lymphoid tissue and peripheral  
66 blood, there are significant proportions of DN T cells among total  $\alpha\beta$  T cells in steady-state as  
67 well as post-AKI kidneys (19). DN T cells exhibited a protective role with an anti-inflammatory  
68 property in prevention from moderate early injury (19), however little is known about their role  
69 in repair after AKI, particularly after clinically significant severe injury. We therefore  
70 hypothesized that kidney DN T cells change after severe AKI and can directly participate in  
71 repair. We studied effects of DN T cells after severe AKI, effects on renal epithelial cells in vitro



72 as well as in vivo AKI, comparing them to the “gold standard” anti-inflammatory CD4<sup>+</sup> Tregs  
73 (18, 20).

74

## 75 **MATERIALS AND METHODS**

### 76 **Mice**

77 Seven-week-old male C57BL/6J wild-type (WT) mice were purchased from Jackson Laboratory  
78 (Bar Harbor, ME) and housed under specific pathogen-free conditions at the Johns Hopkins  
79 University animal facility. 8–9-week-old mice were used for experiments using WT mice. 12-  
80 week-old *Fas<sup>tgld</sup>/J* male mice were used as donors for DN T cell isolation as previously described  
81 (19, 21). All experiments were performed using experimental protocols approved by the Animal  
82 Care and Use Committee of Johns Hopkins University and reported in compliance with the  
83 ARRIVE guideline (22).

84

### 85 **Severe ischemic AKI model**

86 WT mice were anesthetized with pentobarbital (75 mg/kg; Akorn, Lake Forest, IL) injection  
87 intraperitoneally. Mice were placed onto a thermostatically controlled heating table after shaving  
88 of abdominal hair. Abdominal midline incision was performed, and left renal pedicles were  
89 dissected and clamped for 40 min using a microvascular clamp (Roboz Surgical Instrument,  
90 Gaithersburg, MD) to induce severe ischemia. The clamps were released from renal pedicles

91 after 40 min, and the left kidneys were visually inspected to confirm reperfusion. Mice were kept  
92 well hydrated with 1 mL of warm sterile 0.9% saline and at a constant body temperature (37 °C)  
93 during the surgery. After being sutured, mice were allowed to recover with free access to chow  
94 and water.

95

### 96 **Assessment of kidney function**

97 Since serum creatinine is a less sensitive measure of GFR in the unilateral IRI model due to the  
98 remaining functional contralateral kidney (23), we directly measured glomerular filtrate rate  
99 (GFR) to measure kidney function. GFR was measured by transcutaneous fluorescein  
100 isothiocyanate (FITC)-sinistrin (inulin analog) with a fluorometer device (MediBeacon, St. Louis,  
101 MO) at baseline, 24hrs, one week, two weeks, and three weeks after reperfusion (24). Briefly,  
102 mice were anesthetized with isoflurane (Piramal, Maharashtra, India) and oxygen under an  
103 isoflurane vaporizer system (VetFlo, Kent Scientific, Torrington, CT). The background  
104 fluorescence signal of skin was recorded for five minutes, and subsequently 0.07 mg/g body  
105 weight of FITC-sinistrin (MediBeacon) was injected retro-orbitally. Mice were immediately  
106 transferred to separate cages to record FITC-sinistrin clearance in dark. After 1.5 hrs, the devices  
107 were gently detached from conscious mice, and raw data from the devices were collected using  
108 MB Lab Software (MediBeacon). GFR was calculated using a previously established three-  
109 compartment model (25) by Studio2 Software (MediBeacon).

110

111 **Tissue histological analysis**

112 At 3 weeks after the surgery, mice were anesthetized with intraperitoneal injection of ketamine  
113 (130 mg/kg; VetOne, Boise, ID) and xylazine (7 mg/kg; Akorn) mixture. Mice were  
114 exsanguinated, and kidneys were collected. Left kidney tissues were fixed with 10% buffered  
115 formalin followed by paraffin embedding. Kidney sections were subsequently stained with  
116 Masson's trichrome staining. A renal pathologist, blinded to the study groups, scored the degree  
117 of fibrosis from the kidney sections.

118

119 **Isolation of kidney mononuclear cells**

120 For kidney mononuclear cell isolation, post-ischemic kidneys and contralateral kidneys were  
121 collected at 1 week and 3 weeks after the IRI surgery. Uninjured intact kidneys from naïve mice  
122 were also collected for steady state controls. Kidney mononuclear cells (KMNCs) were isolated  
123 using Percoll density gradient protocol described previously (26). Briefly, decapsulated kidneys  
124 were incubated in 2 mg/mL collagenase D (Roche, Basel, Switzerland) solution for 30 min at  
125 37 °C. Samples were strained through 70 µm cell strainer (BD Biosciences, Franklin Lakes, NJ),  
126 washed, and resuspended in 40% Percoll (GE Healthcare, Chicago, IL) followed by gentle  
127 overlaying onto 80% Percoll. After centrifugation at 1,800 g for 30 min in brake-off mode at  
128 room temperature, KMNCs were collected from the interface between 40% and 80% Percoll.  
129 Collected cells were washed and resuspended with Roswell Park Memorial Institute (RPMI)  
130 1640 media (Thermo Fisher Scientific, Waltham, MA) containing 5% fetal bovine serum (FBS,

131 Thermo Fisher Scientific). Cells were counted on a hemocytometer using trypan blue (Thermo  
132 Fisher Scientific) under a microscope (IMT-2, Olympus, Tokyo, Japan).

133

#### 134 **Spectral flow cytometry**

135 Cells were washed once with phosphate buffered saline (PBS) and stained with viability dye  
136 Zombie NIR Fixable Viability (BioLegend, San Diego, CA) for 15 min at room temperature.  
137 After washing with Cell Staining Buffer (BioLegend), cells were preincubated with anti-  
138 CD16/CD32 Fc receptor blocking antibody (S17011E, BioLegend) for 15 min to prevent  
139 nonspecific antibody binding. Subsequently, surface staining was performed with surface  
140 staining antibody cocktail in 50 uL of BD horizon<sup>TM</sup> Brilliant Stain buffer for 30 min at 4 °C:  
141 Pacific blue anti-CD44 (IM7, BioLegend), BV510 anti-CD8 (53-6.7, BioLegend), BV570 anti-  
142 CD45 (30-F11, BioLegend), BV605 anti-CD69 (H1.2F3, BioLegend), BV650 anti-NK1.1  
143 (PK136, BioLegend), BV711 anti-PD1 (29F.1A12, BioLegend), BV785 anti-TCR $\beta$  (H57-597,  
144 BioLegend), Alexa Fluor 532 anti-CD3 (17A2, Thermo Fisher Scientific), PE/Dazzel 594 anti-T-  
145 cell immunoreceptor with Ig and ITIM domains (TIGIT) (1G9, BioLegend), PE-Cy5 anti-CD122,  
146 PE-Cy5.5 anti-CD25 (PC61.5, Thermo Fisher Scientific), PE-Cy7 anti-Ly49 (14B11, BioLegend),  
147 Alexa Fluor 647 anti-TCR $\gamma\delta$  (GL3, BioLegend), APC-R700 anti-CD62L (MEL-14, BD  
148 Biosciences), and APC-Fire810 anti-CD4 (GK1.5, BioLegend). Cells were fixed and  
149 permeabilized with Foxp3/Transcription Factor Staining kit (Thermo Fisher Scientific) for 30  
150 min at room temperature and washed with permeabilization/wash buffer (Thermo Fisher  
151 Scientific). Intracellular staining was conducted in 50 $\mu$ L of permeabilization/wash buffer with

152 intracellular staining antibody cocktail for 30 min at room temperature: BV421 anti-Ki67 (16A8,  
153 BioLegend), PerCP-eFluor 710 anti-FoxP3 (FJK-16S, Thermo Fisher Scientific).

154

### 155 **T cell activation and intracellular cytokine analysis**

156 To measure intracellular cytokines, KMNCs were stimulated with pre-mixed leukocyte  
157 activation cocktail (BioLegend) containing phorbol 12-myristate-13-acetate, ionomycin, and  
158 brefeldin A. After surface staining followed by permeabilization and fixation as described above,  
159 cells were stained with the following intracellular antibodies, BV421 anti-Ki67 (16A8,  
160 BioLegend), Alexa Fluor 488 anti-TNF $\alpha$  (MP6-XT22, Biolegend), Alexa Fluor 532 anti-IL-2  
161 (JES6-5H4, BD Biosciences), PerCP-eFluor 710 anti-FoxP3 (FJK-16S, Thermo Fisher Scientific),  
162 PE anti-IL-10 (JES5-16E3, Biolegend), PE-Cy5 anti-INF $\gamma$  (XMG1.2, Abcam), PE-Cy7 anti-  
163 IL17A (TC11-18H10, Biolegend), Alexa Fluor 647 anti-TGF- $\beta$  (860206, R&D systems,  
164 Minneapolis, MN).

165 After staining, cells were washed with permeabilization/wash buffer then resuspended in Cell  
166 Staining Buffer. Samples were analyzed by 4-laser Aurora spectral flow cytometer (Cytek,  
167 Fremont, CA). The acquired raw data from the spectral flow cytometer were unmixed by  
168 SpectroFlo software (Cytek). Unmixed data was curated and analyzed with FlowJo 10.8 software  
169 (BD Biosciences).

170

### 171 **Double negative T cell sorting**

172 DN T cells were isolated from *gld* mice lymph nodes. Briefly, single-cell suspension of  
173 lymphocytes from lymph nodes was preincubated with anti-CD16/CD32 Fc block (S17011E,  
174 BioLegend) and stained in Cell Staining Buffer (BioLegend) with fluorochrome-labeled  
175 antibodies: APC-Cy7 anti-CD45 (30-F11), BV421 anti-TCR $\beta$  (H57-957), CD4 Alexa Fluor 488  
176 (GK1.5), and CD8 PE (53-6.7) from BioLegend. After staining, cells were washed and  
177 resuspended with BD FACS Pre-Sort Buffer (BD Biosciences). Cells were stained with  
178 propidium iodide (PI) (Thermo Fisher Scientific) right before sorting for viability assay. PI  
179 TCR $\beta^+$  CD4 $^-$  CD8 $^-$  cells were sorted using the MoFlo Legacy or the XDP cell sorter (Beckman  
180 Coulter, Brea, CA).

181

## 182 **Treg and CD4 $^+$ T cell isolation**

183 Tregs and CD4 $^+$  T cells were isolated from WT mouse spleens using CD4 $^+$  CD25 $^+$  Regulatory T  
184 Cell Isolation Kit (Miltenyi Biotec, Bergisch Gladbach, Germany) according to the  
185 manufacturer's protocol. The final eluted fraction containing CD4 $^+$  CD25 $^+$  cells was used as  
186 Treg transfer for both in vitro and in vivo studies. We confirmed that these cells were FoxP3 $^+$   
187 CD4 $^+$  Tregs by flow cytometry analysis before performing adoptive transfer (Supplemental  
188 Figure S1). The flow-through fraction containing CD4 $^+$  CD25 $^-$  T cells was used for CD4 $^+$  T cell  
189 transfer (negative control) for the in vitro scratch experiment.

190

## 191 **In vitro coculture of renal tubular epithelial cells and T cells to quantify repair after injury**

192 The Boston University mouse proximal tubular (BUMPT-306) epithelial cells (PTECs) were  
193 cultured with DMEM with 5% FBS and 100 U/mL penicillin and streptomycin in a 96-well plate  
194 (Sartorius, Niedersachsen, Germany). Cultured cells were exposed to hypoxic condition (1% O<sub>2</sub>)  
195 according to the following protocol. For hypoxia induction, culture plates were placed in a  
196 modular incubator chamber, and the chamber was flushed with gas mixture containing 1% O<sub>2</sub>, 5%  
197 CO<sub>2</sub>, and 94% N<sub>2</sub> for 3 min. Subsequently, the chamber was completely sealed and placed into a  
198 cell culture incubator for 12h.

199 To mimic PTEC repair in vitro, we used a scratch wound assay, a technique used for studying  
200 the effects of cell-cell interactions on cell migration (27). Homogenous scratch wounds were  
201 created to the PTEC monolayer using a 96-pin WoundMaker Tool (Sartorius). Immediately after  
202 scratch, activated DN T cells, CD4<sup>+</sup> Tregs, and CD4<sup>+</sup> T cells were transferred at a 5:1 ratio. Cells  
203 were incubated under normoxia and the phase-contrast images were acquired every 2 hr using a  
204 real-time cell analysis system (Incucyte Live-Cell Analysis, Sartorius). The wound closure was  
205 quantified from time-lapse phase images, and values were expressed as the relative wound  
206 density (Incucyte Scratch Wound Analysis Software Module, Sartorius).

207

## 208 **T cell adoptive transfer**

209 Vehicle, DN T cells or Tregs were injected twice at 6 h and 48 h after reperfusion via retro-  
210 orbital intravenous injection. PBS was used as the vehicle, and isolated cells were resuspended in  
211 PBS right before the injection.  $5 \times 10^6$  DN T cells and  $1 \times 10^6$  Tregs were injected into each mouse  
212 per injection.

213

## 214 **Quantification of mRNA by real-time quantitative reverse transcription PCR**

215 After collecting whole kidneys, the upper 1/3 part of each kidney, which includes cortex and  
216 medulla, was immediately immersed into RNAlater (Thermo Fisher Scientific). These tissues  
217 were subsequently used for RNA isolation followed by RT-PCR. The remaining kidney tissues  
218 were used for lymphocyte isolation for flow cytometry or histologic evaluation. Total RNA was  
219 extracted from kidney tissue with RNeasy Mini kit (Qiagen, Valencia, CA) and reversed  
220 transcribed using high-Capacity cDNA Reverse Transcription Kit (Applied Biosystems,  
221 Waltham, MA). Real-time PCR was performed in QuanStudio 12 Flex (Applied Biosystems)  
222 using the PowerUp SYBR Green Master mix (Applied Biosystems) for detection of mRNA  
223 expression of *Tgfb1*, *Acta2* (encoding  $\alpha$ -smooth muscle actin,  $\alpha$ -SMA), *Colla1*, and *Col4a1*.  
224 *Gapdh* gene expression was used as the internal control. Relative fold expression values were  
225 calculated with a  $\Delta\Delta$  cycle threshold method. The primer sequences for each gene are provided  
226 in Supplemental Table 1.

227

## 228 **Statistics**

229 Data were expressed as mean  $\pm$  standard error of mean (SEM). Two group means were compared  
230 with two-tailed t test. Three or more group means were compared using one-way ANOVA  
231 followed by Tukey's post-hoc analyses. Kruskal-Wallis test followed by Dunn's test was used  
232 for non-normally distributed variables. All statistical analyses were performed using GraphPad



233 Prism version 10 (GraphPad Software, La Jolla, CA). *P* values <0.05 were considered  
234 statistically significant.

235

## 236 **RESULTS**

### 237 **Kidney DN T cells decreased after severe ischemic AKI**

238 Severe unilateral ischemic AKI was induced in mice then DN T cells and other conventional T  
239 cell subsets were evaluated at one week and three weeks after IRI. The gating strategies for  
240 kidney T cells are provided in Supplemental Figure S2. DN T cells significantly decreased  
241 during recovery phase compared to steady-state level by both percentages (Steady state 18.0±0.5%  
242 of αβ T cells; one week 10.1±0.7%, *P*<0.001; three weeks 6.1±0.4%, *P*<0.001) and numbers  
243 ( $3.9 \pm 0.2 \times 10^5$ ;  $2.8 \pm 0.2 \times 10^5$ , *P*=0.006;  $1.2 \pm 0.2 \times 10^5$ , *P*<0.001), whereas CD4<sup>+</sup> Tregs  
244 substantially increased (1.5±0.2%; 7.0±0.3%, *P*<0.001; 14.6±1.1%, *P* <0.001) ( $1.8 \pm 0.2 \times 10^4$ ;  
245  $10.1 \pm 1.0 \times 10^4$ , *P*<0.001;  $15.2 \pm 2.5 \times 10^4$ , *P*<0.001) (Figure 1). Percentages of CD8<sup>+</sup> T cells  
246 increased at one week and three weeks, whereas CD4<sup>+</sup> T cells remained unchanged  
247 (Supplemental Figure S3A). CD8<sup>+</sup> Tregs were also studied given the emerging interest as a  
248 potential regulatory cell (28-30). CD8 Tregs (CD8<sup>+</sup> Ly49<sup>+</sup> CD122<sup>+</sup>) increased at one week and  
249 then decreased at three weeks (Supplemental Figure S3B).

250

### 251 **Activation and proliferation of DN T cells during repair after severe AKI**

252 To study activation and proliferation of DN T cells during AKI recovery, we measured CD44,  
253 CD62L, CD69, and Ki67 expression in DN T cells. Effector memory (EM) phenotype (CD44<sup>hi</sup>  
254 CD62L<sup>lo</sup>) DN T cells decreased (Steady state 92.2±0.5%; one week 70.2±1.1%,  $P<0.001$ ; three  
255 weeks 81.3±2.8%,  $P<0.001$ ), whereas central memory (CM) phenotypes (CD44<sup>hi</sup> CD62L<sup>hi</sup>)  
256 increased (6.5±0.4%; 28.8±1.1%,  $P<0.001$ ; 13.1±2.4%,  $P=0.038$ ) in DN T cells during recovery  
257 phase. Activation marker CD69 was downregulated (99.2±0.1%; 95.9±0.6%,  $P=0.016$ ;  
258 85.5±1.0%,  $P<0.001$ ). DN T cell proliferation decreased during recovery phase (Ki67, 97.8 ±  
259 0.5%; 95.1±0.9%,  $P=0.133$ ; 90.5±1.2%,  $P<0.001$ ) (Figure 2).

260

### 261 **Changes in DN T cell immune checkpoint molecules PD1, TIGIT as well as NK1.1 during** 262 **repair after severe AKI**

263 NK1.1<sup>+</sup> and PD1<sup>+</sup> DN T cells are known to be two major subsets of kidney DN T cells (31).  
264 NK1.1 expression (33.4±2.9%; 53.3±1.6%,  $P<0.001$ , 50.4±2.0,  $P<0.001$ ) and PD1 expression  
265 (1.4±0.1%; 1.8±0.2%,  $P=0.820$ ; 3.3±0.7,  $P=0.020$ ) were upregulated at 3 weeks by percentages.  
266 However, the absolute numbers of the DN T cells with positive expression of NK1.1 or PD1 did  
267 not increase due to decreased total DN T cell numbers. A newly recognized immune checkpoint  
268 molecule with a role in early AKI, TIGIT, was also measured (32), and we found TIGIT  
269 expression in DN T cells was decreased (1.9±0.2%; 2.3±0.3%,  $P=0.461$ ; 0.9±0.2,  $P=0.010$ ) at 3  
270 weeks after AKI (Figure 3).

271

272 **DN T cell phenotypes were distinct from CD4<sup>+</sup> and CD8<sup>+</sup> T cells after severe AKI**

273 Immunologic phenotypes of DN T cells were compared with conventional CD4<sup>+</sup> and CD8<sup>+</sup> T  
274 cells 3 weeks after severe AKI. DN T cells had more central-memory (CD44<sup>hi</sup> CD62L<sup>hi</sup>)  
275 phenotype compared to CD4<sup>+</sup> and CD8<sup>+</sup> T cells (DN, 13.1±2.4%; CD4, 2.4±0.2% *P*<0.001; CD8,  
276 1.8±0.1%, *P*<0.001) (Figure 4A). When CD44 and CD62L expression was compared with the  
277 contralateral normal kidneys, DN T cells from post-AKI kidneys showed lower effector-memory  
278 (CD44<sup>hi</sup> CD62L<sup>lo</sup>) and higher central-memory (CD44<sup>hi</sup> CD62L<sup>hi</sup>) subtypes compared to those  
279 from the non-ischemic kidneys, whereas CD4<sup>+</sup> and CD8<sup>+</sup> T cells exhibited opposite trends  
280 (Figure 4B). In non-ischemic kidneys, there were substantial percentages of naïve phenotypes in  
281 CD4<sup>+</sup> and CD8<sup>+</sup> T cells, but not in DN T cells. There were few naïve phenotypes in post-  
282 ischemic kidneys in DN, CD4<sup>+</sup>, and CD8<sup>+</sup> T cells (Figure 4B).

283 DN T cell Ki67 expression was lower compared to CD4<sup>+</sup> and CD8<sup>+</sup> T cells during post-AKI  
284 repair (90.8±1.1%; 94.4±0.3%, *P*=0.001; 95.0±0.6%, *P*=0.001) (Figure 4C). CD69 expression in  
285 DN T cells from post-ischemic kidneys was lower compared to those of non-ischemic kidneys  
286 while CD8<sup>+</sup> T cells showed the opposite trend. Ki67 expression was lower in CD4<sup>+</sup> and CD8<sup>+</sup> T  
287 cells from non-ischemic kidneys compared to those from ischemic kidneys, whereas it was  
288 consistently high in both non-ischemic and post-ischemic kidneys in DN T cells (Figure 4D).

289 DN T cell NK1.1 expression was substantially higher than CD4<sup>+</sup> and CD8<sup>+</sup> T cells, and PD1 and  
290 TIGIT expression was lower than CD4<sup>+</sup> T cells (Supplemental Figure S4).

291

## 292 **Cytokine production by DN T cells after severe AKI**

293 Intracellular cytokine analysis of DN T cells was performed after severe AKI. After 3 weeks  
294 from severe AKI, DN T cells from postischemic kidneys had significantly lower expression of  
295 inflammatory cytokines including IL-17A, IFN- $\gamma$ , and TNF- $\alpha$ , compared to CD4<sup>+</sup> and CD8<sup>+</sup> T  
296 cells. Profibrotic cytokine TGF- $\beta$ 1 expression was also lower in DN T cells than in CD4<sup>+</sup> and  
297 CD8<sup>+</sup> T cells (Figure 5). When cytokine expression was compared with the contralateral non-  
298 ischemic kidneys, there were no significant changes in proinflammatory cytokines in the DN T  
299 cells, whereas there was upregulation of IL-17A, IFN- $\gamma$ , and TNF- $\alpha$  in the CD4<sup>+</sup> or CD8<sup>+</sup> T cells.  
300 TGF- $\beta$ 1 was upregulated in DN T cells from postischemic kidneys than those from nonischemic  
301 kidneys. IL-10 remained unchanged after severe AKI (Figure 5). When IL-10 and TGF- $\beta$ 1  
302 expression was compared between DN T cells and Tregs from postischemic kidneys, IL-10 was  
303 lower in DN T cells whereas TGF- $\beta$ 1 was higher (Supplemental Figure S5).

304

## 305 **DN T cells accelerated proximal tubular epithelial cell repair in vitro**

306 To assess the role of DN T cells in post-AKI repair in vitro, we tested the effect of DN T cell  
307 coculture with tubular epithelial cells. PTECs were cultured and then exposed to hypoxia  
308 followed by normoxia to model ischemia-reperfusion injury in vitro. After creating consistently  
309 sized scratch wounds to tubular epithelial cell monolayer (27), DN T cells were transferred. DN  
310 T cells isolated from *gld* donors were used as commonly performed since large numbers of cells  
311 are required (19, 21, 33). *gld* DN T cells are known to be similar to kidney DN T cells, and they  
312 are capable to suppress T cell proliferation in vitro (33). Tregs were used as a positive control,

313 and CD25<sup>-</sup> CD4<sup>+</sup> T cells were used as an additional negative control to exclude nonspecific effect  
314 of coculturing with lymphocytes. Kinetic quantification was performed with live-cell analysis  
315 system. Cellular density at the wound significantly increased in tubular cells treated with DN T  
316 cells or Tregs, whereas CD4<sup>+</sup> T cell-treated cells did not, compared to the vehicle-treated group  
317 (Figure 6).

318

### 319 **Adoptive transfer of DN T cells after severe AKI increased GFR and decreased kidney** 320 **fibrosis**

321 Given the significant decline of DN T cell numbers in post-severe AKI kidneys and in vitro  
322 ability of DN T cells to enhance tubular epithelial cell repair, we performed in vivo adoptive  
323 transfer experiments to evaluate whether the DN T cell replenishment could reduce kidney  
324 fibrosis and enhance renal recovery. DN T cells isolated from *gld* donors were adoptively  
325 transferred at 6h and 48h after reperfusion. We previously demonstrated that adoptively  
326 transferred *gld* DN T cells migrate into kidneys (19). CD4 Tregs were also transferred as a  
327 positive control. Mice underwent serial GFR measurements during 3-week follow-up. Fibrosis  
328 was measured from kidney histology sections, and profibrotic gene expression was quantified at  
329 3 weeks after AKI. Kidney T cells were also studied using flow cytometry (Figure 7A). The  
330 gating strategy for DN T cell sorting is provided in Supplemental Figure S6.

331 We found significant increases in GFR after 3 weeks from ischemic AKI in DN T cell  
332 transferred groups and Treg transferred group (Vehicle 976.7±29.0  $\mu$ L/min/100 g; DN T cells  
333 1092.0±31.4  $\mu$ L/min/100 g,  $P=0.012$ ; Tregs 1104.9±42.5  $\mu$ L/min/100 g,  $P=0.021$ ) (Figure 7B).

334 Mice treated with DN T cells exhibited reduced medullary fibrosis (vehicle 76.3±3.2%. DN T  
335 cells, 58.1±3.3%,  $P=0.008$ ; Tregs 48.7±5.7%,  $P<0.001$ ) compared to the vehicle control group.  
336 There were no significant differences in cortex (vehicle 57.4±4.5%; DN T cells 45.8±2.6%,  
337  $P=0.176$ ; Tregs 41.4±6.0%,  $P=0.051$ ) (Figure 7C).

338 We found that kidney expression of profibrotic genes *Tgfb* (Vehicle 1.46±0.14; DN T cells  
339 1.02±0.07,  $P=0.011$ ; Tregs 0.92±0.10,  $P=0.003$ ) and *Acta2* (encoding  $\alpha$ -SMA) (Vehicle  
340 1.66±0.15; DN T cells 1.22±0.09,  $P=0.033$ ; Tregs 1.13±0.12,  $P=0.014$ ) were reduced in the DN  
341 T cell-treated group and Treg-treated group. *Colla1* was decreased in the Treg transfer group  
342 (Vehicle 1.56±0.15; DN T cells 1.24±0.15,  $P=0.190$ ; Tregs 1.07±0.12,  $P=0.043$ ). *Col4a1* was  
343 comparable between groups (Vehicle 1.53±0.14; DN T cells 1.36±0.10,  $P=0.527$ ; Tregs  
344 1.30±0.11,  $P=0.381$ ) (Figure 7D).

345

### 346 **DN T cells decrease kidney effector T cells and their IL-17A expression**

347 To begin to elucidate mechanisms by which DN T cells improved GFR and decreased kidney  
348 fibrosis after severe AKI, we studied kidney T cells from post-ischemic kidneys at 3 weeks.  
349 Although the proportions and numbers of CD4<sup>+</sup>, CD8<sup>+</sup>, and DN T cells were comparable  
350 between the groups, we found percentages and numbers of effector-memory CD4<sup>+</sup> T cells were  
351 lower in the DN T cell and Treg-treated groups compared to the vehicle-treated group (Vehicle  
352 96.9±0.3%; DN T cells 94.7±0.2%,  $P<0.001$ ; Tregs 93.7±0.3%,  $P=0.021$ ) (Figure 8A). We also  
353 measured cytokine expression on kidney CD4<sup>+</sup> T cells and found that IL-17A expression was  
354 reduced in DN T cell and Treg-treated groups (Vehicle 7.0±1.3%; 3.0±0.4%,  $P=0.008$ ; 2.8±0.5,

355  $P=0.020$ ) (Figure 8B). The other cytokines remain unchanged. Thus, a potential mechanism by  
356 which DN T cell reduces kidney fibrosis through decreased effector T cells and IL-17A.

357

## 358 **DISCUSSION**

359 Based on previous data that Tregs mediate organ repair (34) and emerging data on the important  
360 role of kidney DN T cells in prevention of AKI (19, 21, 31), we hypothesized that DN T cells  
361 undergo functional changes during recovery and could have a reparative role after severe  
362 ischemic AKI. Analysis of kidney T cells after severe ischemic AKI using tissue digestion and  
363 spectral flow cytometry demonstrated that DN T cells decrease substantially during the repair  
364 phase and undergo long-term distinct immunologic changes compared to kidney  $CD4^+$ ,  $CD8^+$ ,  
365 and  $CD4^+$  Tregs. DN T cell coculture enhanced tubular epithelial cell repair following injury.  
366 Addition of DN T cells to injured renal tubular epithelial cells *in vitro* accelerated wound repair  
367 comparable to the “gold” standard Tregs. Adoptive transfer of DN T cells administered after  
368 severe AKI increased GFR and reduced kidney fibrosis, as well as reduced effector-memory  
369  $CD4^+$  T cells and IL-17A expression.

370 DN T cells are rare in lymphoid organs and peripheral blood, but they constitute significant  
371 proportions of kidney  $TCR\alpha\beta^+$  T cells both in mice and human kidneys (17-20). It was thought  
372 that DN T cells originated from  $CD4^+$  or  $CD8^+$  T cells by loss of receptors, however kidney  
373  $TCR\alpha\beta^+$  DN T cells were identified in mice lacking  $CD4^+$  T cells (MHC II-deficient mice) and  
374 those lacking  $CD8^+$  T cells ( $\beta 2m$ -deficient mice), which suggest DN T cells can be derived from  
375 distinct progenitors (31). Kidney DN T cells expand early after moderate AKI kidneys within the

376 first 24 h, and then rapidly decrease at 72h below the steady-state level (19). In the present study,  
377 we found that kidney DN T cells significantly decrease both in numbers and proportion at later  
378 time points until 3 weeks after severe AKI. Interestingly, DN T cell kinetics during the AKI  
379 repair were opposite to CD4<sup>+</sup> Tregs that showed marked expansion (15, 16, 19, 31).

380 Though we studied Tregs as a “positive control” anti-inflammatory cell, we found a significant  
381 expansion of CD8<sup>+</sup> Tregs (CD8<sup>+</sup> CD122<sup>+</sup> Ly49<sup>+</sup>), a relatively understudied T cell subset, during  
382 repair after severe AKI. The expansion of CD8<sup>+</sup> Tregs has also been demonstrated by a recent  
383 study using a cerebral IRI model (35). Emerging evidence suggests that CD8<sup>+</sup> CD122<sup>+</sup> Tregs are  
384 involved in immune regulation as their counterpart, CD4<sup>+</sup> Tregs (28, 29). Given the recent  
385 promising data showing the protective role against other organ IRI (35), CD8<sup>+</sup> Tregs’ role in  
386 AKI is a promising topic of future study.

387 Previous studies have shown that DN T cells had distinct immunophenotypical features during  
388 early injury compared to kidney CD4<sup>+</sup> and CD8<sup>+</sup> T cells (19, 31). In the present study, we  
389 observed late immunologic changes toward more central-memory phenotypes with less  
390 proliferation rather than effector-memory phenotypes, an opposing trend with CD4<sup>+</sup> and CD8<sup>+</sup> T  
391 cells during post-AKI recovery. These long-term changes and distinct kinetics/phenotype of DN  
392 T cells, compared to Tregs, CD4<sup>+</sup>, and CD8<sup>+</sup> cells, compose the complex immune response to  
393 repair and fibrosis after severe AKI.

394 Consistent with our earlier findings showing that PD1<sup>+</sup> subset is a potent early responder in  
395 ischemic AKI (31), we observed increased expression of the PD1<sup>+</sup> during the recovery phase  
396 after severe AKI as well. However, the absolute number of PD1<sup>+</sup> DN T remained comparable to  
397 normal kidneys due to the substantial decline in the total number of DN T cells despite PD1



398 upregulation. Besides PD1 expression, we also studied a novel immune checkpoint molecule,  
399 TIGIT, given the recent data on its importance on AKI (32). In contrast to upregulation of TIGIT  
400 during the early injury phase (32), TIGIT<sup>+</sup> DN T cells decreased during the recovery phase.  
401 Considering the important role of immune checkpoint molecules in AKI (32, 36, 37) and  
402 continued clinical experience of checkpoint inhibitor-associated AKI in cancer patients (38), we  
403 believe that findings from our current study have potential clinical relevance.

404 Proximal tubular epithelial cells are a primary target of ischemic injury and previous studies have  
405 demonstrated direct interactions between these cells and T cells in vitro (11). We therefore  
406 investigated the reparative capacity of DN T cells by co-culturing them with wounded PTECs.  
407 DN T cells significantly enhanced wound healing capacity of PTECs following hypoxic injury.  
408 Thus, there could be DN T cell-driven reparative mediators, affecting tubular epithelial cells,  
409 which needs to be further explored.

410 Although the immunologic mechanisms of long-term injury after AKI are less understood than  
411 early injury, chronic T cell expansion is frequently seen during AKI repair and fibrosis (12, 13).  
412 More specifically, CD4<sup>+</sup> T cells skewed toward effector-memory phenotype with upregulated  
413 activation markers (12, 13). Taken together with the findings from other organ fibrosis models  
414 (39, 40), chronic proinflammatory T cell activation is likely to have an important role in kidney  
415 fibrosis and CKD transition. Inhibition of late CD4<sup>+</sup> T cell activation could be a potential  
416 therapeutic target to reduce kidney fibrosis and CKD transition. In the present study, we  
417 observed that post-AKI DN T cell repletion reduced effector-memory CD4<sup>+</sup> T cells, consistent  
418 with previously found CD4<sup>+</sup> T cell suppressive function (19). Another important finding was that  
419 DN T cells reduced IL-17 expression in CD4<sup>+</sup> T cells. IL-17 and IL-17-producing T cells were

420 suggested as important contributors to AKI and CKD transition (41-43). There was an increase  
421 of IL-17 expressing T cells during post-AKI repair, and genes related to IL-17 pathway were  
422 upregulated in kidney fibrosis (14). Elevated IL-17 expression was observed in kidney biopsy  
423 specimens from patients with kidney fibrosis (44). Blocking IL-17<sup>+</sup> cell activation or deletion of  
424 *Il17* gene mitigated renal injury (41-43). Taken together, the reparative effect of DN T cells  
425 could be attributed to inhibiting effector CD4<sup>+</sup> T cells and IL-17 downregulation. Since the IL-17  
426 downregulation was observed in CD4<sup>+</sup> Treg-treated group as well, the IL-17-dependent  
427 mechanism could also be involved in the well-known protective effect of Treg-based therapy  
428 (45).

429 The immunoregulatory role of DN T cells has also been shown in other chronic disease models  
430 such as allograft rejection, graft-versus-host disease, and type 1 diabetes (46). However, DN T  
431 cells' proinflammatory pathogenic roles have also been reported particularly in autoimmune  
432 diseases such as lupus, psoriasis, and Sjogren syndrome (47). These discordant findings are  
433 likely due to their heterogeneity or plasticity (48). For example, a recent study using single-cell  
434 RNA sequencing analysis proposed 5 different subsets of DN T cells (49). Discovering a specific  
435 marker for reparative DN T cell subset is needed for a deeper understanding of this population.

436 The current study has several limitations. First, although we focused on T cell-mediated  
437 mechanisms in AKI repair, other types of kidney immune cells such as macrophages, dendritic  
438 cells, neutrophils, B cells, and innate lymphoid cells could also play important roles in AKI  
439 repair (50-52). Thus, we cannot rule out a collateral effect of DN T cells on other types of kidney  
440 immune cells. Second, there are currently no available DN T cell specific markers, thus we were  
441 unable to deplete kidney DN T cells or use models lacking DN T cells. The discovery of

442 reparative kidney DN T cell-specific markers is warranted for future studies to use these  
443 techniques to further understand the role of DN T cells. Another limitation was that we used *gld*  
444 DN T cells, which are not identical to WT DN T cells. However, since DN T cells are rarely  
445 present in lymphoid organs, it is challenging to get enough DN T cells for DN T cell adoptive  
446 transfer. We previously demonstrated that adoptively transferred *gld* DN T cells migrate into  
447 post-AKI kidneys (19).

448 Despite these limitations, our study is novel and has important pathophysiologic and therapeutic  
449 implications. The decreasing kinetics of DN T cells could be a potential target involved in kidney  
450 fibrosis in other diseases. Cell immunotherapy is an increasing reality, particularly for cancer  
451 patients. The regulatory cell-based therapy field has flourished with recent ongoing clinical trials  
452 in kidney diseases (53). The present study identifies a novel therapeutic approach to administer  
453 expanded DN T cells to accelerate recovery and decrease fibrosis in patients after severe AKI.

454

455 **DATA AVAILABILITY**

456 The data that support the findings of this study are available from the corresponding author upon  
457 reasonable request.

458

459 **SUPPLEMENTAL MATERIAL**

460 **Supplemental Figure S1. Flow cytometry analysis of sorted Tregs for adoptive transfer**  
461 **study.**

462 **Supplemental Figure S2. Gating strategies for kidney T cells.**

463 **Supplemental Figure S3. Changes in CD4<sup>+</sup>, CD8<sup>+</sup> T cells and CD8<sup>+</sup> Tregs during repair**  
464 **phase after severe ischemic AKI.**

465 **Supplemental Figure S4. Differences in NK1.1 and immune checkpoint molecule expression**  
466 **between DN, CD4<sup>+</sup>, and CD8<sup>+</sup> T cells after severe AKI.**

467 **Supplemental Figure S5. IL-10 and TGF-β1 expression in DN T cells and Tregs from**  
468 **postischemic kidneys.**

469 **Supplemental Figure S6. Gating strategy for DN T cell sorting from *gld* donors.**

470 **Supplemental Table 1. Primer sequences for profibrotic genes.**

471 **Supplemental Material link: <https://doi.org/10.6084/m9.figshare.24547087>**

472 **ACKNOWLEDGMENTS**

473 We thank Gregg L. Semenza's lab of JHU School of Medicine for providing hypoxic incubator  
474 and helping with in vitro hypoxia experiments. We also thank Hao Zhang of Johns Hopkins  
475 Bloomberg School of Public Health and Hyun Jun Jung of JHU School of Medicine for their  
476 technical support. We would like to acknowledge the JHU Ross Flow Cytometry Core Facility  
477 (S10OD026859) for help in this study.

478 K.L. was supported by grants from Korea Health Industry Development Institute (HI19C1337),  
479 National Research Foundation of Korea (NRF-2021R1A6A3A03039863), Samsung Medical  
480 Center Grant (SMO1230251), and the Young Investigator Research Grant from the Korean  
481 Nephrology Research Foundation (2023). J.T.K. was supported by the Dr. Werner Jackstädt-  
482 Foundation award (S 134–10.117). A.N.R. was supported by the National Institute of Diabetes  
483 and Digestive and Kidney Diseases (NIDDK) PAR-21-071 Diversity Research Supplement  
484 (3R01DK123342-03S1). S.N. was supported by Carl W. Gottschalk Research Scholar Grant  
485 from the American Society of Nephrology (134535), Edward S Kraus award from the Johns  
486 Hopkins School of Medicine Division of Nephrology, National Kidney Foundation Serving  
487 Maryland and Delaware mini-grant (142076), and NIDDK grants (R01DK132278,  
488 R01DK123342, R01DK104662). H.R. was supported by the NIDDK grants (R01DK104662 and  
489 R01DK123342).

490 BioRender.com software was used in generating some of the illustrations.

491

492 **GRANTS**

493 National Institutes of Health, National Institute of Diabetes and Digestive and Kidney Diseases,  
494 R01DK104662 (to H.R.)

495

#### 496 **DISCLOSURES**

497 Authors declare no conflict of interest.

498

#### 499 **AUTHOR CONTRIBUTIONS**

500 H.R. designed the study. K.L. and H.R. drafted the manuscript. K.L., S.G., J.T.K., A.N.R, and  
501 S.N. performed the experiments. K.L., S.N., and H.R. analyzed and interpreted the data. L.J.A.  
502 analyzed histology data. S.G., J.T.K, A.N.R., L.J.A, and S.N. revised the manuscript. All authors  
503 approved the final version of the manuscript.

504

## 505 REFERENCES

506

- 507 1. **Kellum JA, Romagnani P, Ashuntantang G, Ronco C, Zarbock A, Anders HJ.** Acute  
508 kidney injury. *Nat Rev Dis Primers* 7: 52, 2021. doi:10.1038/s41572-021-00284-z
- 509 2. **Chawla LS, Eggers PW, Star RA, Kimmel PL.** Acute kidney injury and chronic kidney  
510 disease as interconnected syndromes. *N Engl J Med* 371: 58-66, 2014.  
511 doi:10.1056/NEJMra1214243
- 512 3. **Jang HR, Rabb H.** Immune cells in experimental acute kidney injury. *Nat Rev Nephrol* 11:  
513 88-101, 2015. doi:10.1038/nrneph.2014.180
- 514 4. **Thomas ME, Blaine C, Dawnay A, Devonald MA, Ftouh S, Laing C, Latchem S,  
515 Lewington A, Milford DV, Ostermann M.** The definition of acute kidney injury and its  
516 use in practice. *Kidney Int* 87: 62-73, 2015. doi:10.1038/ki.2014.328
- 517 5. **Aufhauser DD, Jr., Wang Z, Murken DR, Bhatti TR, Wang Y, Ge G, Redfield RR, 3rd,  
518 Abt PL, Wang L, Svoronos N, Thomasson A, Reese PP, Hancock WW, Levine MH.**  
519 Improved renal ischemia tolerance in females influences kidney transplantation outcomes. *J*  
520 *Clin Invest* 126: 1968-1977, 2016. doi:10.1172/JCI84712
- 521 6. **Bonventre JV, Yang L.** Cellular pathophysiology of ischemic acute kidney injury. *J Clin*  
522 *Invest* 121: 4210-4221, 2011. doi:10.1172/JCI45161
- 523 7. **Wei Q, Sun H, Song S, Liu Y, Liu P, Livingston MJ, Wang J, Liang M, Mi QS, Huo Y,  
524 Nahman NS, Mei C, Dong Z.** MicroRNA-668 represses MTP18 to preserve mitochondrial  
525 dynamics in ischemic acute kidney injury. *J Clin Invest* 128: 5448-5464, 2018.  
526 doi:10.1172/JCI121859
- 527 8. **Yang L, Besschetnova TY, Brooks CR, Shah JV, Bonventre JV.** Epithelial cell cycle  
528 arrest in G2/M mediates kidney fibrosis after injury. *Nat Med* 16: 535-543, 531p following  
529 143, 2010. doi:10.1038/nm.2144
- 530 9. **Ying WZ, Li X, Rangarajan S, Feng W, Curtis LM, Sanders PW.** Immunoglobulin light  
531 chains generate proinflammatory and profibrotic kidney injury. *J Clin Invest* 129: 2792-  
532 2806, 2019. doi:10.1172/JCI125517
- 533 10. **Burne MJ, Daniels F, El Ghandour A, Mauiyyedi S, Colvin RB, O'Donnell MP, Rabb  
534 H.** Identification of the CD4+ T cell as a major pathogenic factor in ischemic acute renal  
535 failure. *J Clin Invest* 108: 1283-1290, 2001. doi:10.1172/JCI12080
- 536 11. **Rabb H, Daniels F, O'Donnell M, Haq M, Saba SR, Keane W, Tang WW.**  
537 Pathophysiological role of T lymphocytes in renal ischemia-reperfusion injury in mice. *Am J*  
538 *Physiol Renal Physiol* 279: F525-531, 2000. doi:10.1152/ajprenal.2000.279.3.F525
- 539 12. **Burne-Taney MJ, Yokota N, Rabb H.** Persistent renal and extrarenal immune changes  
540 after severe ischemic injury. *Kidney Int* 67: 1002-1009, 2005. doi:10.1111/j.1523-  
541 1755.2005.00163.x
- 542 13. **Ascon M, Ascon DB, Liu M, Cheadle C, Sarkar C, Racusen L, Hassoun HT, Rabb H.**  
543 Renal ischemia-reperfusion leads to long term infiltration of activated and effector-memory  
544 T lymphocytes. *Kidney Int* 75: 526-535, 2009. doi:10.1038/ki.2008.602

- 545 14. **do Valle Duraes F, Lafont A, Beibel M, Martin K, Darribat K, Cuttat R, Waldt A,**  
546 **Naumann U, Wieczorek G, Gaulis S, Pfister S, Mertz KD, Li J, Roma G, Warncke M.**  
547 Immune cell landscaping reveals a protective role for regulatory T cells during kidney injury  
548 and fibrosis. *JCI Insight* 5: 2020. doi:10.1172/jci.insight.130651
- 549 15. **Kinsey GR, Huang L, Vergis AL, Li L, Okusa MD.** Regulatory T cells contribute to the  
550 protective effect of ischemic preconditioning in the kidney. *Kidney Int* 77: 771-780, 2010.  
551 doi:10.1038/ki.2010.12
- 552 16. **Gandolfo MT, Jang HR, Bagnasco SM, Ko GJ, Agreda P, Satpute SR, Crow MT, King**  
553 **LS, Rabb H.** Foxp3+ regulatory T cells participate in repair of ischemic acute kidney injury.  
554 *Kidney Int* 76: 717-729, 2009. doi:10.1038/ki.2009.259
- 555 17. **Ascon DB, Ascon M, Satpute S, Lopez-Briones S, Racusen L, Colvin RB, Soloski MJ,**  
556 **Rabb H.** Normal mouse kidneys contain activated and CD3+CD4- CD8- double-negative T  
557 lymphocytes with a distinct TCR repertoire. *J Leukoc Biol* 84: 1400-1409, 2008.  
558 doi:10.1189/jlb.0907651
- 559 18. **Crispin JC, Oukka M, Bayliss G, Cohen RA, Van Beek CA, Stillman IE, Kyttaris VC,**  
560 **Juang YT, Tsokos GC.** Expanded double negative T cells in patients with systemic lupus  
561 erythematosus produce IL-17 and infiltrate the kidneys. *J Immunol* 181: 8761-8766, 2008.  
562 doi:10.4049/jimmunol.181.12.8761
- 563 19. **Martina MN, Noel S, Saxena A, Bandapalle S, Majithia R, Jie C, Arend LJ, Allaf ME,**  
564 **Rabb H, Hamad AR.** Double-Negative alphabeta T Cells Are Early Responders to AKI and  
565 Are Found in Human Kidney. *J Am Soc Nephrol* 27: 1113-1123, 2016.  
566 doi:10.1681/ASN.2014121214
- 567 20. **Li H, Adamopoulos IE, Moulton VR, Stillman IE, Herbert Z, Moon JJ, Sharabi A,**  
568 **Krishfield S, Tsokos MG, Tsokos GC.** Systemic lupus erythematosus favors the generation  
569 of IL-17 producing double negative T cells. *Nat Commun* 11: 2859, 2020.  
570 doi:10.1038/s41467-020-16636-4
- 571 21. **Gong J, Noel S, Hsu J, Bush EL, Arend LJ, Sadasivam M, Lee SA, Kurzhagen JT,**  
572 **Hamad ARA, Rabb H.** TCR(+)CD4(-)CD8(-) (double negative) T cells protect from  
573 cisplatin-induced renal epithelial cell apoptosis and acute kidney injury. *Am J Physiol Renal*  
574 *Physiol* 318: F1500-F1512, 2020. doi:10.1152/ajprenal.00033.2020
- 575 22. **Kilkenny C, Browne WJ, Cuthill IC, Emerson M, Altman DG.** Improving bioscience  
576 research reporting: the ARRIVE guidelines for reporting animal research. *PLoS Biol* 8:  
577 e1000412, 2010. doi:10.1371/journal.pbio.1000412
- 578 23. **Fu Y, Tang C, Cai J, Chen G, Zhang D, Dong Z.** Rodent models of AKI-CKD transition.  
579 *Am J Physiol Renal Physiol* 315: F1098-F1106, 2018. doi:10.1152/ajprenal.00199.2018
- 580 24. **Scarfe L, Schock-Kusch D, Ressel L, Friedemann J, Shulhevich Y, Murray P, Wilm B,**  
581 **de Caestecker M.** Transdermal Measurement of Glomerular Filtration Rate in Mice. *J Vis*  
582 *Exp* 2018. doi:10.3791/58520
- 583 25. **Friedemann J, Heinrich R, Shulhevich Y, Raedle M, William-Olsson L, Pill J, Schock-**  
584 **Kusch D.** Improved kinetic model for the transcutaneous measurement of glomerular  
585 filtration rate in experimental animals. *Kidney Int* 90: 1377-1385, 2016.  
586 doi:10.1016/j.kint.2016.07.024



- 587 26. **Ascon DB, Lopez-Briones S, Liu M, Ascon M, Savransky V, Colvin RB, Soloski MJ,**  
588 **Rabb H.** Phenotypic and functional characterization of kidney-infiltrating lymphocytes in  
589 renal ischemia reperfusion injury. *J Immunol* 177: 3380-3387, 2006.  
590 doi:10.4049/jimmunol.177.5.3380
- 591 27. **Liang CC, Park AY, Guan JL.** In vitro scratch assay: a convenient and inexpensive  
592 method for analysis of cell migration in vitro. *Nat Protoc* 2: 329-333, 2007.  
593 doi:10.1038/nprot.2007.30
- 594 28. **Kim HJ, Wang X, Radfar S, Sproule TJ, Roopenian DC, Cantor H.** CD8+ T regulatory  
595 cells express the Ly49 Class I MHC receptor and are defective in autoimmune prone B6-  
596 Yaa mice. *Proc Natl Acad Sci U S A* 108: 2010-2015, 2011. doi:10.1073/pnas.1018974108
- 597 29. **Dai Z, Zhang S, Xie Q, Wu S, Su J, Li S, Xu Y, Li XC.** Natural CD8+CD122+ T cells are  
598 more potent in suppression of allograft rejection than CD4+CD25+ regulatory T cells. *Am J*  
599 *Transplant* 14: 39-48, 2014. doi:10.1111/ajt.12515
- 600 30. **Cantor H, Kim HJ.** A new chapter in the CD8 T reg story. *J Exp Med* 218: 2021.  
601 doi:10.1084/jem.20201746
- 602 31. **Sadasivam M, Noel S, Lee SA, Gong J, Allaf ME, Pierorazio P, Rabb H, Hamad ARA.**  
603 Activation and Proliferation of PD-1(+) Kidney Double-Negative T Cells Is Dependent on  
604 Nonclassical MHC Proteins and IL-2. *J Am Soc Nephrol* 30: 277-292, 2019.  
605 doi:10.1681/ASN.2018080815
- 606 32. **Noel S, Lee K, Gharai S, Kurzhagen JT, Pierorazio PM, Arend LJ, Kuchroo VK,**  
607 **Cahan P, Rabb H.** Immune Checkpoint Molecule TIGIT Regulates Kidney T Cell  
608 Functions and Contributes to AKI. *J Am Soc Nephrol* 34: 755-771, 2023.  
609 doi:10.1681/asn.0000000000000063
- 610 33. **Hamad AR, Mohamood AS, Trujillo CJ, Huang CT, Yuan E, Schneck JP.** B220+  
611 double-negative T cells suppress polyclonal T cell activation by a Fas-independent  
612 mechanism that involves inhibition of IL-2 production. *J Immunol* 171: 2421-2426, 2003.  
613 doi:10.4049/jimmunol.171.5.2421
- 614 34. **D'Alessio FR, Kurzhagen JT, Rabb H.** Reparative T lymphocytes in organ injury. *J Clin*  
615 *Invest* 129: 2608-2618, 2019. doi:10.1172/JCI124614
- 616 35. **Cai W, Shi L, Zhao J, Xu F, Dufort C, Ye Q, Yang T, Dai X, Lyu J, Jin C, Pu H, Yu F,**  
617 **Hassan S, Sun Z, Zhang W, Hitchens TK, Shi Y, Thomson AW, Leak RK, Hu X, Chen**  
618 **J.** Neuroprotection against ischemic stroke requires a specific class of early responder T  
619 cells in mice. *J Clin Invest* 132: 2022. doi:10.1172/JCI157678
- 620 36. **Schoop R, Wahl P, Le Hir M, Heemann U, Wang M, Wuthrich RP.** Suppressed T-cell  
621 activation by IFN-gamma-induced expression of PD-L1 on renal tubular epithelial cells.  
622 *Nephrol Dial Transplant* 19: 2713-2720, 2004. doi:10.1093/ndt/gfh423
- 623 37. **Jaworska K, Ratajczak J, Huang L, Whalen K, Yang M, Stevens BK, Kinsey GR.** Both  
624 PD-1 ligands protect the kidney from ischemia reperfusion injury. *J Immunol* 194: 325-333,  
625 2015. doi:10.4049/jimmunol.1400497
- 626 38. **Cortazar FB, Marrone KA, Troxell ML, Ralto KM, Hoenig MP, Brahmer JR, Le DT,**  
627 **Lipson EJ, Glezerman IG, Wolchok J, Cornell LD, Feldman P, Stokes MB, Zapata SA,**

- 628 **Hodi FS, Ott PA, Yamashita M, Leaf DE.** Clinicopathological features of acute kidney  
629 injury associated with immune checkpoint inhibitors. *Kidney Int* 90: 638-647, 2016.  
630 doi:10.1016/j.kint.2016.04.008
- 631 39. **Bresser P, Jansen HM, Weller FR, Lutter R, Out TA.** T-cell activation in the lungs of  
632 patients with systemic sclerosis and its relation with pulmonary fibrosis. *Chest* 120: 66s-68s,  
633 2001. doi:10.1378/chest.120.1\_suppl.s66
- 634 40. **Luzina IG, Atamas SP, Wise R, Wigley FM, Choi J, Xiao HQ, White B.** Occurrence of  
635 an activated, profibrotic pattern of gene expression in lung CD8+ T cells from scleroderma  
636 patients. *Arthritis Rheum* 48: 2262-2274, 2003. doi:10.1002/art.11080
- 637 41. **Chan AJ, Alikhan MA, Odobasic D, Gan PY, Khouri MB, Steinmetz OM, Mansell AS,**  
638 **Kitching AR, Holdsworth SR, Summers SA.** Innate IL-17A-producing leukocytes  
639 promote acute kidney injury via inflammasome and Toll-like receptor activation. *Am J*  
640 *Pathol* 184: 1411-1418, 2014. doi:10.1016/j.ajpath.2014.01.023
- 641 42. **Mehrotra P, Collett JA, McKinney SD, Stevens J, Ivancic CM, Basile DP.** IL-17  
642 mediates neutrophil infiltration and renal fibrosis following recovery from ischemia  
643 reperfusion: compensatory role of natural killer cells in athymic rats. *Am J Physiol Renal*  
644 *Physiol* 312: F385-F397, 2017. doi:10.1152/ajprenal.00462.2016
- 645 43. **Mehrotra P, Sturek M, Neyra JA, Basile DP.** Calcium channel Orail promotes  
646 lymphocyte IL-17 expression and progressive kidney injury. *J Clin Invest* 129: 4951-4961,  
647 2019. doi:10.1172/JCI126108
- 648 44. **Coppock GM, Aronson LR, Park J, Qiu C, Park J, DeLong JH, Radaelli E, Susztak K,**  
649 **Hunter CA.** Loss of IL-27 $\alpha$  Results in Enhanced Tubulointerstitial Fibrosis  
650 Associated with Elevated Th17 Responses. *J Immunol* 205: 377-386, 2020.  
651 doi:10.4049/jimmunol.1901463
- 652 45. **Sawitzki B, Harden PN, Reinke P, Moreau A, Hutchinson JA, Game DS, Tang Q,**  
653 **Guinan EC, Battaglia M, Burlingham WJ, Roberts ISD, Streitz M, Josien R, Böger CA,**  
654 **Scottà C, Markmann JF, Hester JL, Juerchott K, Braudeau C, James B, Contreras-**  
655 **Ruiz L, van der Net JB, Bergler T, Caldara R, Petchey W, Edinger M, Dupas N,**  
656 **Kapinsky M, Mutzbauer I, Otto NM, Öllinger R, Hernandez-Fuentes MP, Issa F,**  
657 **Ahrens N, Meyenberg C, Karitzky S, Kunzendorf U, Knechtle SJ, Grinyó J, Morris PJ,**  
658 **Brent L, Bushell A, Turka LA, Bluestone JA, Lechler RI, Schlitt HJ, Cuturi MC,**  
659 **Schlickeiser S, Friend PJ, Miloud T, Scheffold A, Secchi A, Crisalli K, Kang SM,**  
660 **Hilton R, Banas B, Blanco G, Volk HD, Lombardi G, Wood KJ, Geissler EK.**  
661 Regulatory cell therapy in kidney transplantation (The ONE Study): a harmonised design  
662 and analysis of seven non-randomised, single-arm, phase 1/2A trials. *Lancet* 395: 1627-1639,  
663 2020. doi:10.1016/s0140-6736(20)30167-7
- 664 46. **Juvet SC, Zhang L.** Double negative regulatory T cells in transplantation and  
665 autoimmunity: recent progress and future directions. *J Mol Cell Biol* 4: 48-58, 2012.  
666 doi:10.1093/jmcb/mjr043
- 667 47. **Li H, Tsokos GC.** Double-negative T cells in autoimmune diseases. *Curr Opin Rheumatol*  
668 33: 163-172, 2021. doi:10.1097/bor.0000000000000778

- 669 48. **Newman-Rivera AM, Kurzhagen JT, Rabb H.** TCRalpha+ CD4-/CD8- "double  
670 negative" T cells in health and disease-implications for the kidney. *Kidney Int* 102: 25-37,  
671 2022. doi:10.1016/j.kint.2022.02.035
- 672 49. **Yang L, Zhu Y, Tian D, Wang S, Guo J, Sun G, Jin H, Zhang C, Shi W, Gershwin ME,**  
673 **Zhang Z, Zhao Y, Zhang D.** Transcriptome landscape of double negative T cells by single-  
674 cell RNA sequencing. *J Autoimmun* 121: 102653, 2021. doi:10.1016/j.jaut.2021.102653
- 675 50. **Lee SA, Noel S, Sadasivam M, Hamad ARA, Rabb H.** Role of Immune Cells in Acute  
676 Kidney Injury and Repair. *Nephron* 137: 282-286, 2017. doi:10.1159/000477181
- 677 51. **Kung CW, Chou YH.** Acute kidney disease: an overview of the epidemiology,  
678 pathophysiology, and management. *Kidney Res Clin Pract* 42: 686-699, 2023.  
679 doi:10.23876/j.krcp.23.001
- 680 52. **Wang C, Li SW, Zhong X, Liu BC, Lv LL.** An update on renal fibrosis: from mechanisms  
681 to therapeutic strategies with a focus on extracellular vesicles. *Kidney Res Clin Pract* 42:  
682 174-187, 2023. doi:10.23876/j.krcp.22.159
- 683 53. **Rabb H, Lee K, Parikh CR.** Beyond kidney dialysis and transplantation: what's on the  
684 horizon? *J Clin Invest* 132: 2022. doi:10.1172/jci159308
- 685

686 **FIGURE LEGENDS**

687

688 **Figure 1. Changes in anti-inflammatory T cells during repair phase after severe AKI.**

689 DN T cells significantly decreased after severe ischemic AKI by percentages and numbers,  
690 whereas CD4<sup>+</sup> Tregs markedly increased. Statistical analyses were performed using one-way  
691 ANOVA followed by Tukey's post hoc analysis ( $n = 8$  for steady state kidneys,  $n = 10$  for 1  
692 week,  $n = 11$  for 3 weeks). Data are from 3 independent experiments.  $*P < 0.05$ ;  $**P < 0.01$ ;  
693  $***P < 0.001$ . The steady state group refers to uninjured normal kidneys from naïve control mice.  
694 AKI, acute kidney injury; DN, double-negative; IRI, ischemia-reperfusion injury; Treg,  
695 regulatory T cells.

696

697 **Figure 2. Double-negative T cell activation and proliferation during repair phase after**  
698 **severe AKI.**

699 Effector-memory (CD44<sup>hi</sup> CD62L<sup>lo</sup>) DN T cells decreased significantly after severe AKI during  
700 repair, whereas percentages of central-memory (CD44<sup>hi</sup> CD62L<sup>hi</sup>) DN T cells increased.  
701 Expression of markers for activation (CD69) and proliferation (Ki67) decreased significantly in  
702 DN T cells during repair phase. Statistical analyses were performed using one-way ANOVA  
703 followed by Tukey's post hoc analysis ( $n = 8$  for steady state kidneys,  $n = 10$  for 1 week,  $n = 11$   
704 for 3 weeks). Data are from 3 independent experiments.  $*P < 0.05$ ;  $**P < 0.01$ ;  $***P < 0.001$ .  
705 The steady state group refers to uninjured normal kidneys from naïve control mice.  
706 AKI, acute kidney injury; CM, central-memory; DN, double-negative; EM, effector-memory;  
707 IRI, ischemia-reperfusion injury.

708

709 **Figure 3. Changes in NK1.1 and immune checkpoint molecules in double-negative T cells in**  
710 **the repair phase after severe AKI.**

711 NK1.1 and PD1 expression was upregulated at 3 weeks by percentages, whereas TIGIT  
712 expression was decreased at 3 weeks after AKI. Statistical analyses were performed using one-  
713 way ANOVA followed by Tukey's post hoc analysis ( $n = 8$  for steady state kidneys,  $n = 10$  for 1  
714 week,  $n = 11$  for 3 weeks). Data are from 3 independent experiments.  $*P < 0.05$ ;  $**P < 0.01$ ;  
715  $***P < 0.001$ . The steady state group refers to uninjured normal kidneys from naïve control mice.  
716 AKI, acute kidney injury; IRI, ischemia-reperfusion injury; TIGIT, T-cell immunoreceptor with  
717 Ig and ITIM domains.

718

719 **Figure 4. Phenotypical differences between double-negative T cells, CD4<sup>+</sup> and CD8<sup>+</sup> T cells**  
720 **3 weeks after severe AKI.**

721 **(A)** DN T cell CD44 and CD62L expression was compared with CD4<sup>+</sup> and CD8<sup>+</sup> T cells at 3  
722 weeks after severe ischemic AKI. DN T cells had a lower effector-memory phenotype (CD44<sup>hi</sup>  
723 CD62L<sup>lo</sup>) compared to CD4<sup>+</sup> T cells during post-AKI repair. There were few central-memory  
724 phenotypes (CD44<sup>hi</sup> CD62L<sup>hi</sup>) in CD4<sup>+</sup> and CD8<sup>+</sup> T cells. **(B)** When CD44 and CD62L  
725 expression was compared to the contralateral normal kidneys, DN T cells from post-AKI kidneys  
726 had lower effector-memory and higher central-memory phenotypes compared to those from the  
727 contralateral normal kidneys. CD4<sup>+</sup> and CD8<sup>+</sup> T cells showed opposite trends. There were few  
728 naïve phenotype T cells in post-AKI kidneys. Only CD4<sup>+</sup> and CD8<sup>+</sup> T cells had substantial naïve  
729 phenotypes in normal kidneys, and they decreased in the post-AKI kidneys. **(C)** Ki67 expression

730 among three different T cell subsets was compared in post-AKI kidneys at 3 weeks. CD8<sup>+</sup> T cells  
731 had the highest expression of CD69. Ki67 expression was lower in the DN T cells compared to  
732 CD4<sup>+</sup> and CD8<sup>+</sup> T cells. **(D)** When CD69 and Ki67 expression was compared to the  
733 corresponding subsets from the contralateral normal kidneys, CD69 was lower in the DN T cells  
734 from post-AKI kidneys than those from contralateral normal kidneys. Ki69 was higher in CD4<sup>+</sup>  
735 and CD8 T<sup>+</sup> cells from the post-AKI kidneys, whereas DN T cell Ki67 expression remained  
736 unchanged. Statistical analyses were performed using one-way ANOVA followed by Tukey's  
737 post hoc analysis ( $n = 11$ ). Data are from 3 independent experiments. \* $P < 0.05$ ; \*\* $P < 0.01$ ;  
738 \*\*\* $P < 0.001$ . The empty bars and grey bars represent T cells from ischemic and non-ischemic  
739 (uninjured contralateral) kidneys, respectively.

740 AKI, acute kidney injury; CM, central-memory; DN, double-negative; EM, effector-memory.

741

742 **Figure 5. Cytokine production by DN T cells during repair phase after severe AKI.**

743 Expression of inflammatory cytokines, IL-17A, IFN- $\gamma$ , and TNF- $\alpha$ , was significantly lower in  
744 DN T cells than CD4<sup>+</sup> and CD8<sup>+</sup> T cells 3 weeks after severe AKI. TGF- $\beta$ 1 was lower in DN T  
745 cells compared to CD4<sup>+</sup> and CD8<sup>+</sup> T cells. Compared to the corresponding subsets from the  
746 contralateral non-ischemic kidneys, IL-17A increased in CD4<sup>+</sup> T cells, and IFN- $\gamma$  and TNF- $\alpha$   
747 increased in CD8<sup>+</sup> T cells, whereas IL-17, IFN- $\gamma$ , and TNF- $\alpha$  remained unchanged in DN T cells.  
748 TGF- $\beta$ 1 expression was higher in all T cell subsets from postischemic kidneys compared to those  
749 from non-ischemic kidneys. Statistical analyses were performed using one-way ANOVA  
750 followed by Tukey's post hoc analysis ( $n = 16$ ). Data are from 3 independent experiments. \* $P <$   
751  $0.05$ ; \*\* $P < 0.01$ ; \*\*\* $P < 0.001$ . The empty bars and grey bars represent T cells from ischemic  
752 and non-ischemic kidneys, respectively.

753 AKI, acute kidney injury; DN, double-negative; IL, interleukin; IFN, interferon; TGF,  
754 transforming growth factor; TNF, tumor necrosis factor.

755

756 **Figure 6. Double-negative T cell coculture accelerated kidney tubular epithelial cell repair**  
757 **in vitro.**

758 Scratch wounds were created to proximal tubular epithelial cell monolayer after hypoxia  
759 exposure. Activated DN T cells, Tregs (positive control), CD4<sup>+</sup> T cells (negative control), or  
760 vehicle (negative control) were transferred after scratch. Phase-contrast images were acquired  
761 serially using a live-cell analysis system. **(A)** Representative wound images at 24h with  
762 segmentation lines shown for the initial scratch (blue) and wound (yellow). **(B)** Kinetic  
763 quantification showing percent wound density for DN, Tregs, CD4<sup>+</sup> T cells, vehicle, and  
764 normoxia control groups. The normoxia control group showed higher wound density compared  
765 to the other groups exposed to hypoxia ( $P < 0.05$  for all time points). DN T cell coculture  
766 exhibited better wound repair compared to the Vehicle and CD4<sup>+</sup> T cell coculture groups (at 24h,  
767 vehicle  $56.3 \pm 2.1\%$ ; CD4  $56.1 \pm 1.2\%$ , vs vehicle  $P > 0.999$ ; DN  $67.5 \pm 2.3\%$ , vs vehicle  $P = 0.007$ ,  
768 vs CD4  $P = 0.006$ ; Tregs  $62.1 \pm 3.0\%$ , vs vehicle,  $P = 0.275$ , vs CD4,  $P = 0.250$ ).  $n = 8$  replicates  
769 /group. Statistical analyses were performed using one-way ANOVA followed by Tukey's post  
770 hoc analysis.  $*P < 0.05$  compared to the vehicle control group

771 DN, double-negative; Tregs, regulatory T cells.

772

773 **Figure 7. Double-negative T cell treatment after severe AKI increased GFR and reduced**  
774 **kidney fibrosis.**

775 (A) Schematic of experimental design. DN T cells, Vehicle (negative control), or Tregs (positive  
776 control) were adoptively transferred after severe ischemic AKI. GFR was measured with FITC-  
777 sinistrin-based method. Kidney sections were stained with Masson's trichrome to assess kidney  
778 fibrosis. Fibrosis genes were quantified with quantitative RT-PCR. Kidney T cells were isolated  
779 and studied by spectral flow cytometry. (B) GFRs at 3 weeks were higher in the DN T cell ( $n =$   
780 17) and Treg ( $n = 14$ ) transfer groups than the vehicle control group ( $n = 17$ ). (C) Masson's  
781 trichrome staining at 3 weeks after severe AKI. Kidney fibrosis in outer medullar was  
782 significantly lower in the DN T cell-treated group than the vehicle control group ( $n = 9$  /group).  
783 (D) Expression of genes encoding TGF- $\beta$  and  $\alpha$ SMA was lower in the DN T cell-treated group  
784 ( $n = 14$ – $17$  /group). Data are from 3 independent experiments. Statistical analyses were  
785 performed using one-way ANOVA followed by Tukey's post hoc analysis except for GFR data.  
786 The Kruskal-Wallis test followed by Dunn's test was used for GFR due to nonnormal  
787 distribution. \* $P < 0.05$ ; \*\* $P < 0.01$ ; \*\*\* $P < 0.001$ .

788 AKI, acute kidney injury; DN, double-negative; GFR, glomerular filtration rate; Treg, regulatory  
789 T cells.

790

791 **Figure 8. Double-negative T cell adoptive transfer after severe AKI decreased effector**  
792 **CD4<sup>+</sup> T cells and IL-17 production.**

793 T cells from post-AKI kidneys were analyzed at 3 weeks after severe AKI followed by adoptive  
794 transfers. (A) Effector-memory phenotype CD4<sup>+</sup> T cells were lower in the DN T cell and Treg  
795 transfer group.  $n = 10$ – $11$  /group. Data are from 2 independent experiments. (B) IL-17A  
796 expression in CD4<sup>+</sup> T cells was lower in the DN T cell ( $n = 15$ ) and Treg-treated mice ( $n = 9$ )  
797 than in the vehicle control group ( $n = 15$ ). Data are from 3 independent experiments. Statistical



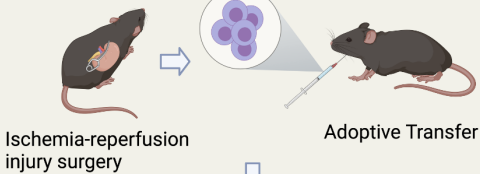
798 analyses were performed using one-way ANOVA followed by Tukey's post hoc analysis. \* $P <$   
799 0.05; \*\* $P < 0.01$ .

800 AKI, acute kidney injury; CM, central-memory; DN, double-negative; EM, effector-memory; IL,  
801 interleukin; Treg, regulatory T cells.

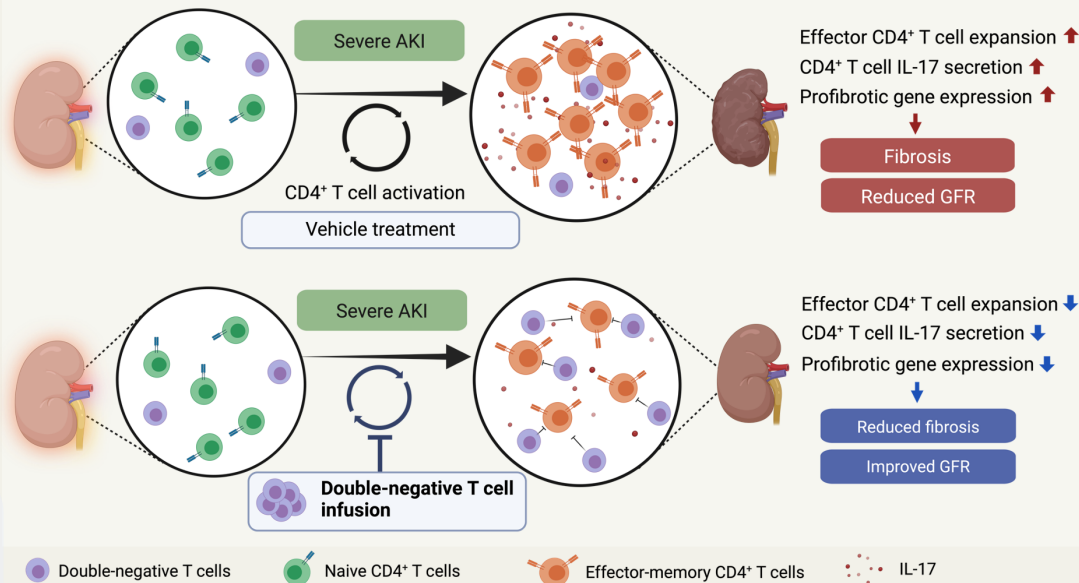
# Double-negative T cells have a reparative role after severe ischemic acute kidney injury

## METHODS

Double-negative T cells

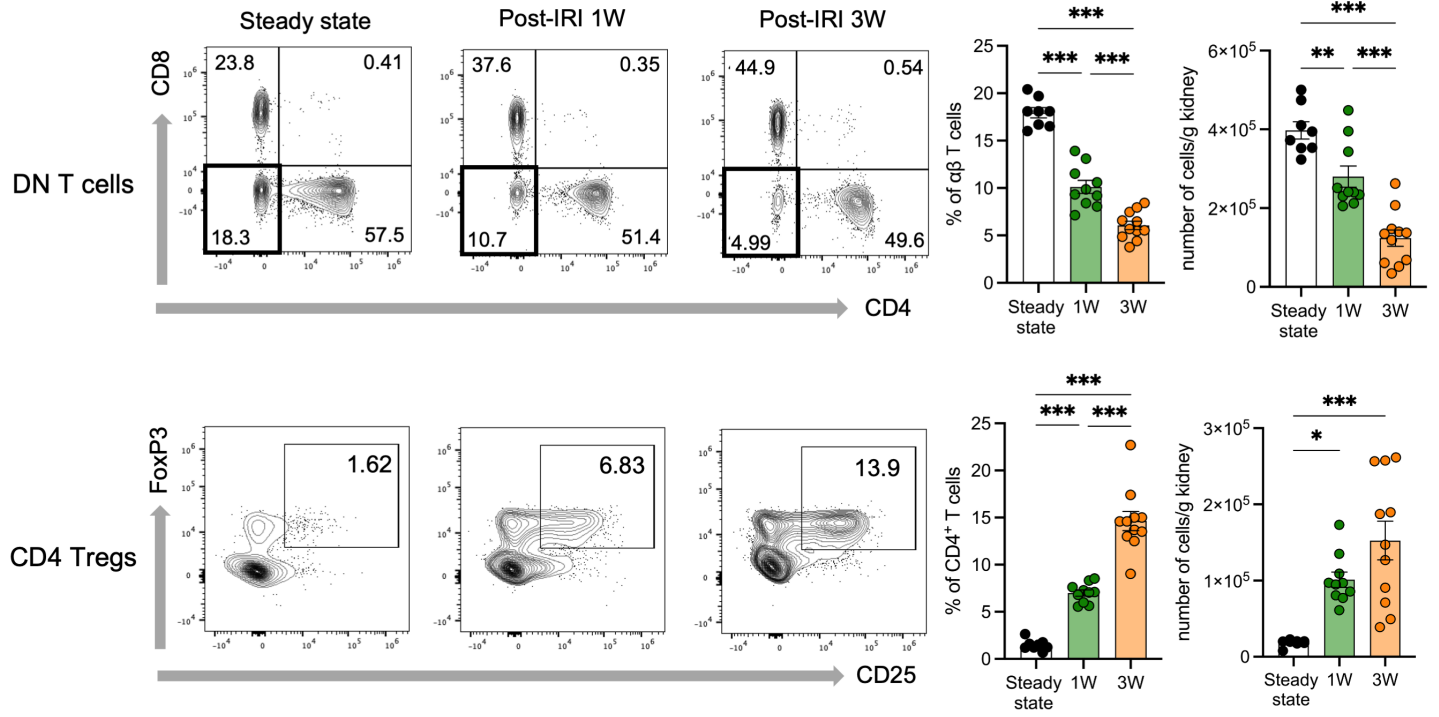


## OUTCOMES

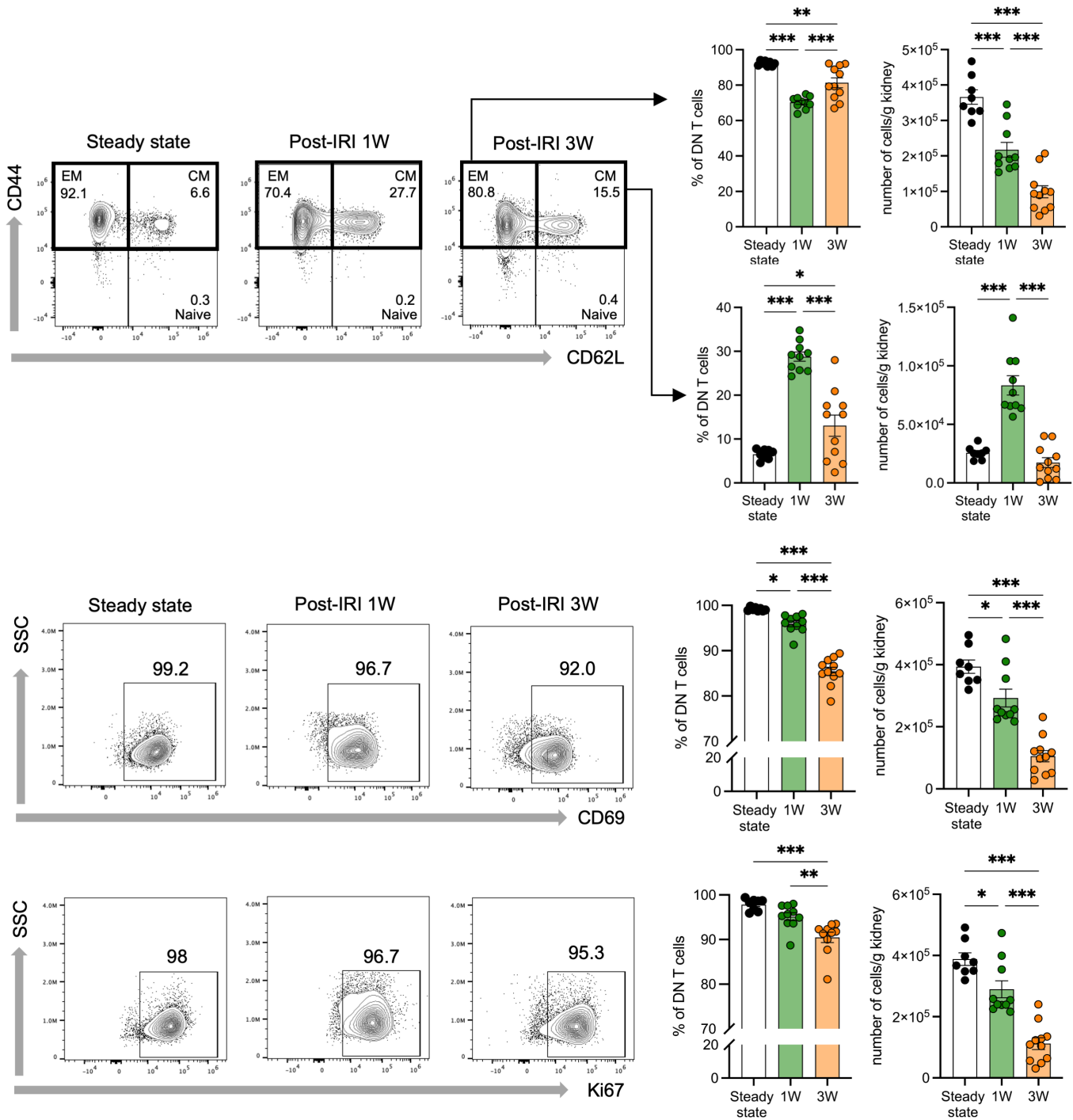


**CONCLUSION** Double-negative T cell infusion after severe AKI improved GFR and decreased renal fibrosis. DN T cells are potential immunotherapy to accelerate repair and mitigate CKD after AKI.

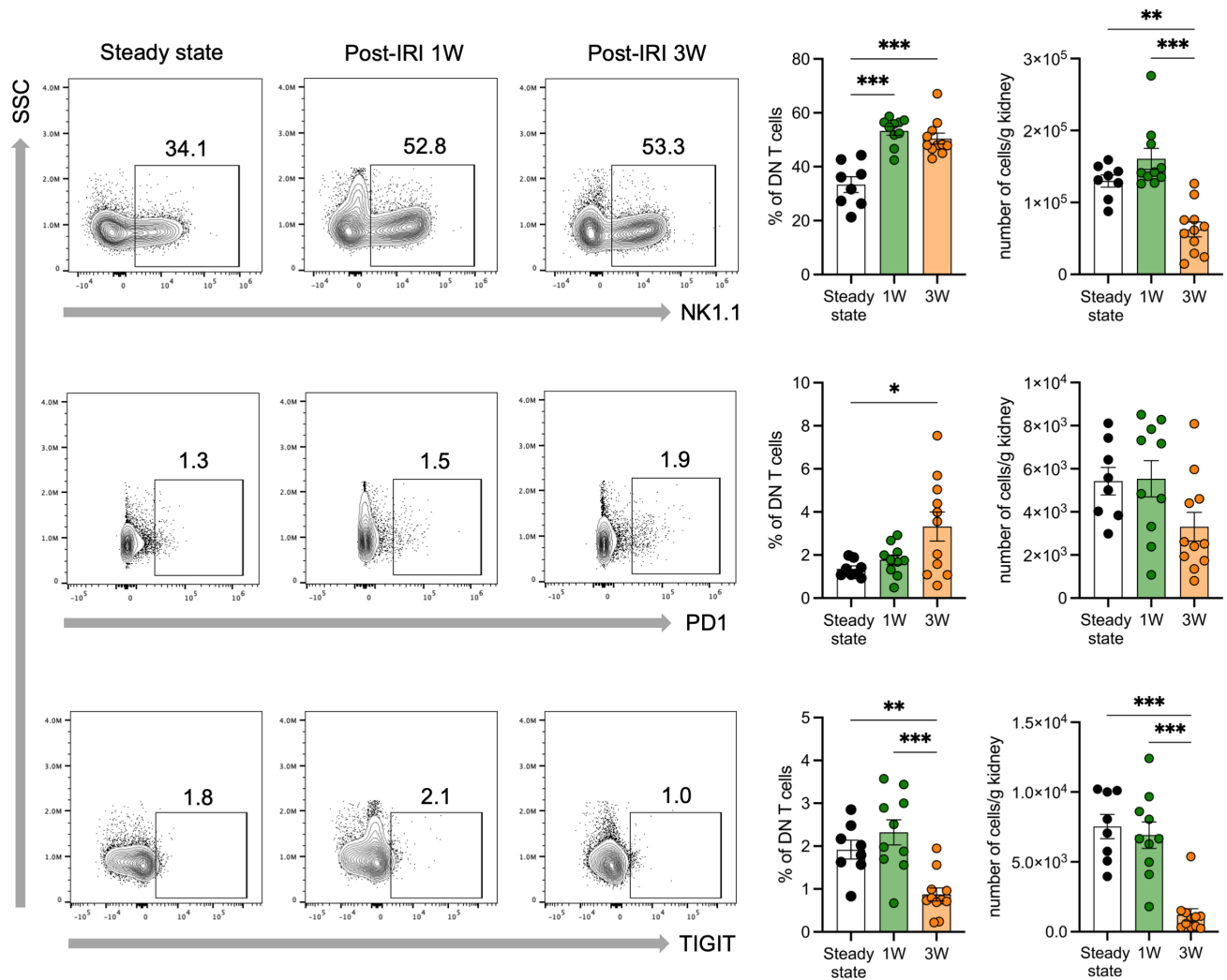
**Figure 1**



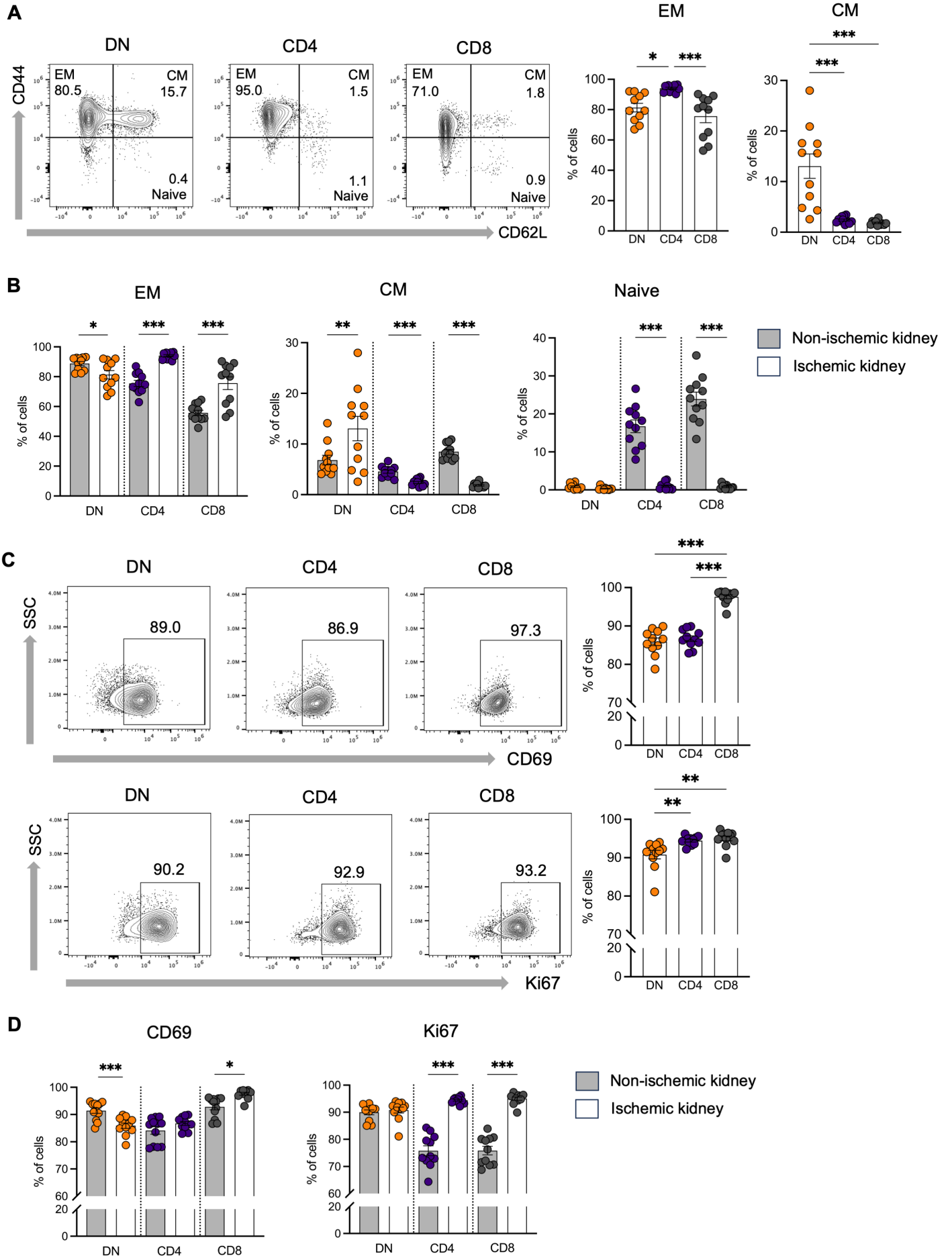
**Figure 2**



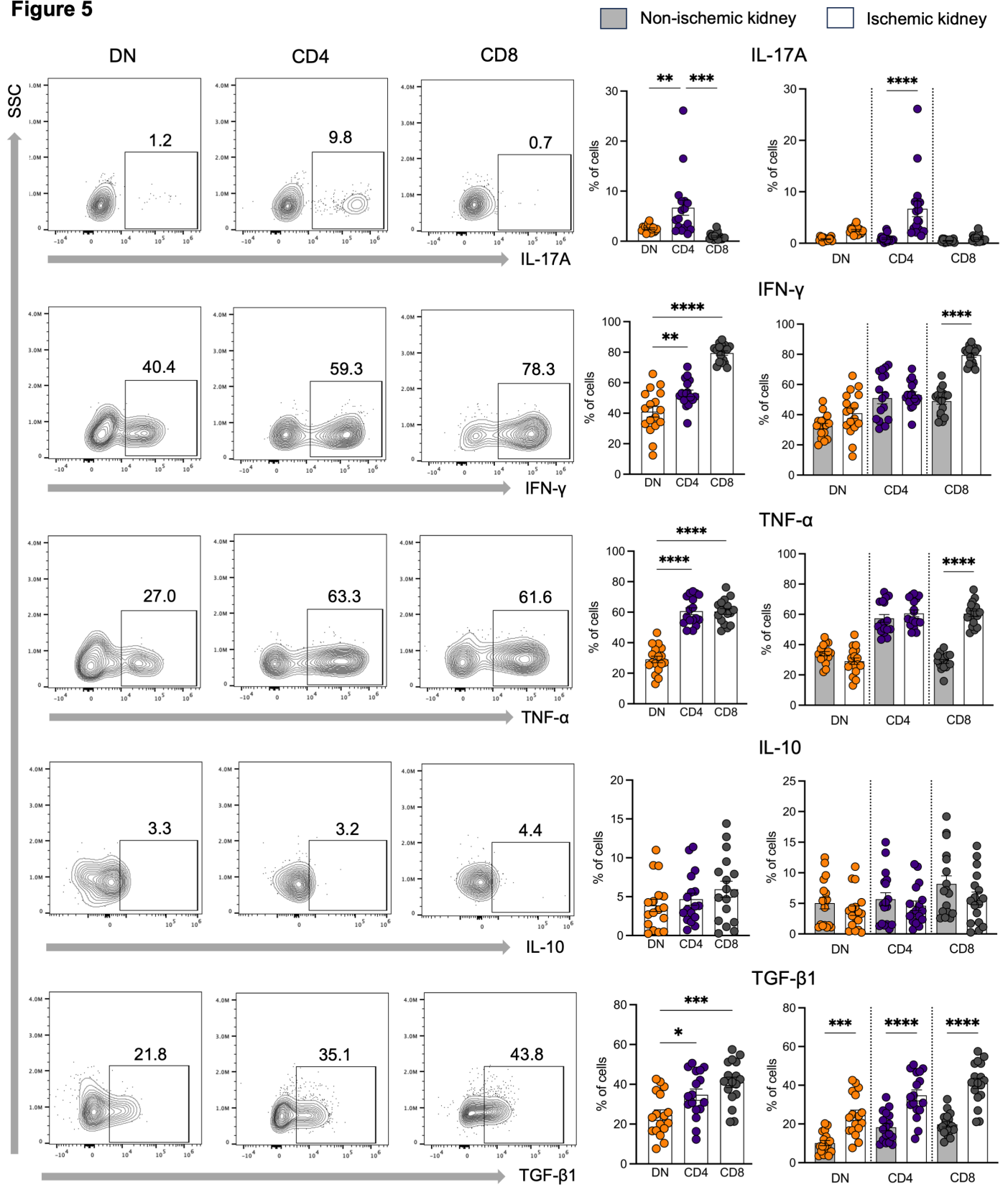
**Figure 3**



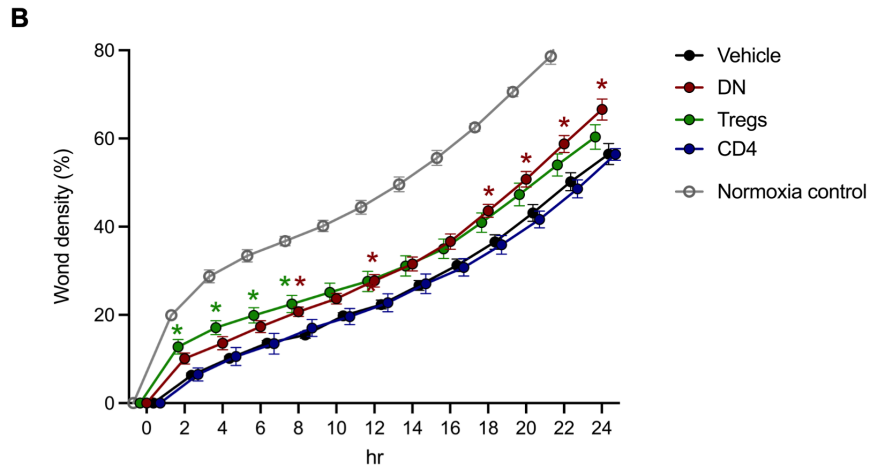
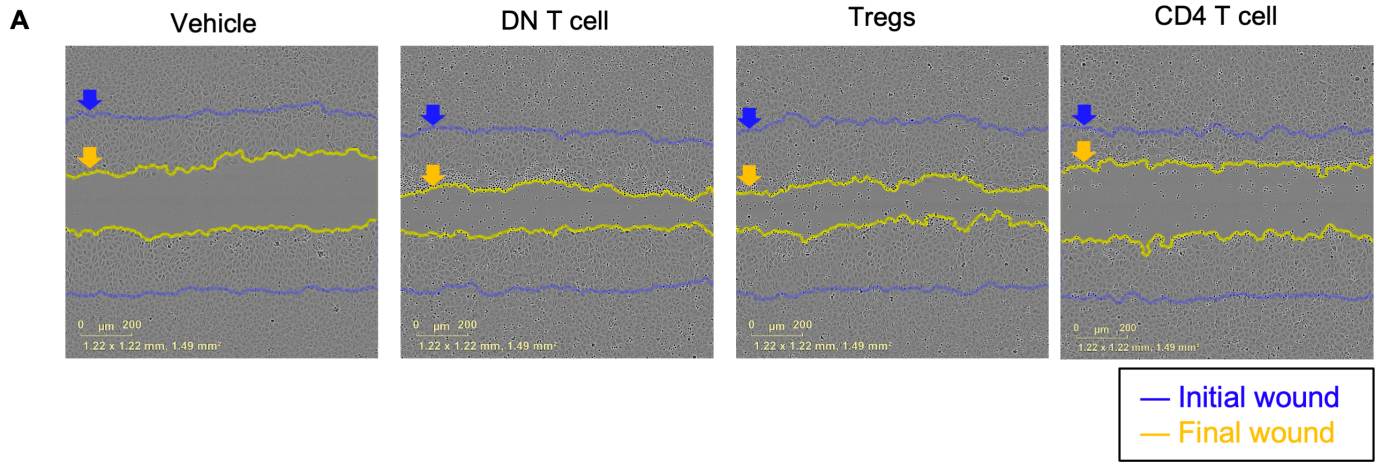
**Figure 4**



**Figure 5**



**Figure 6**





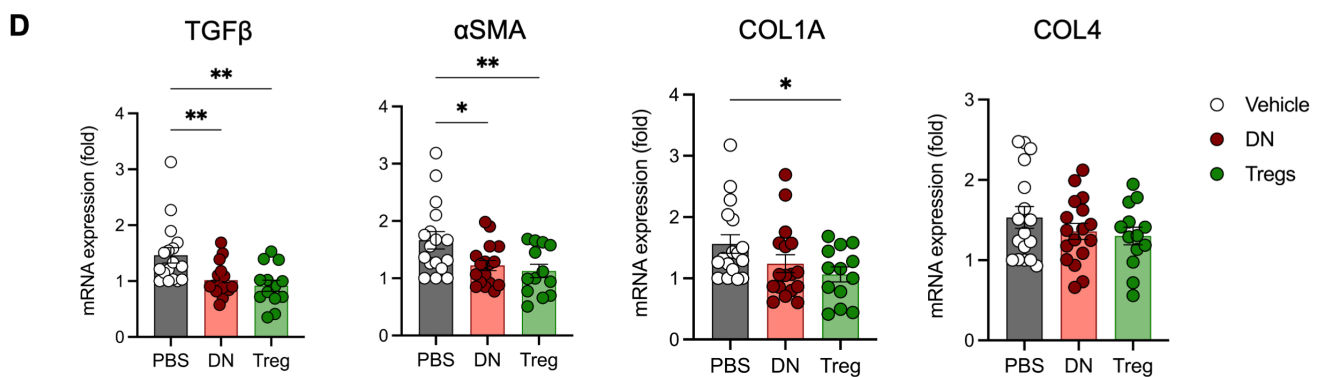
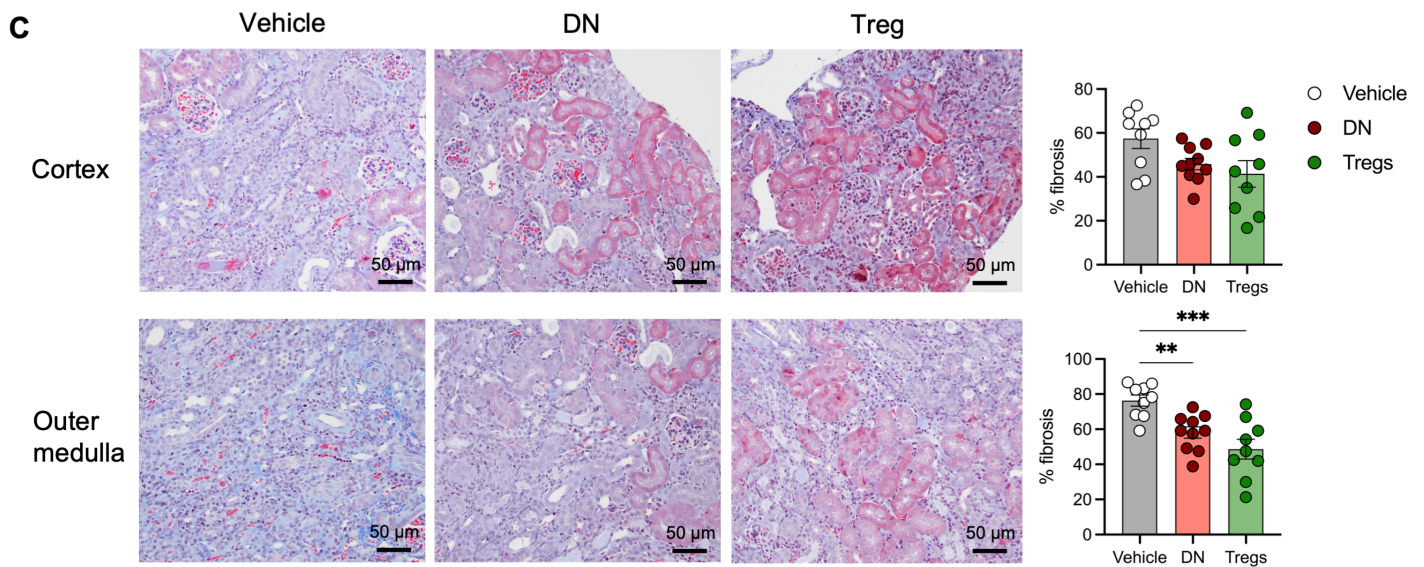
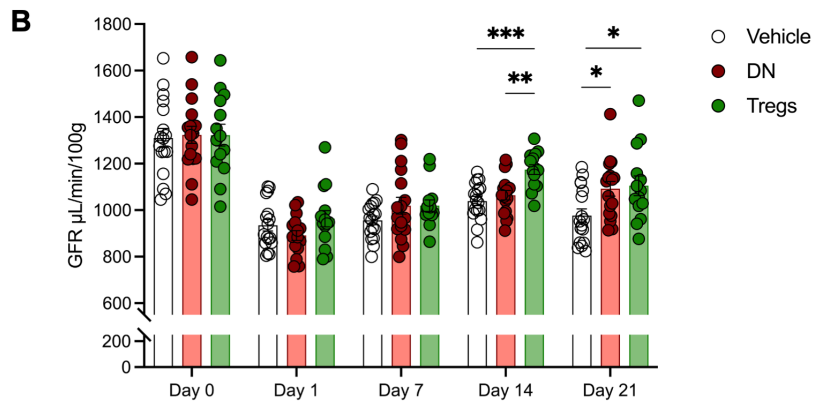
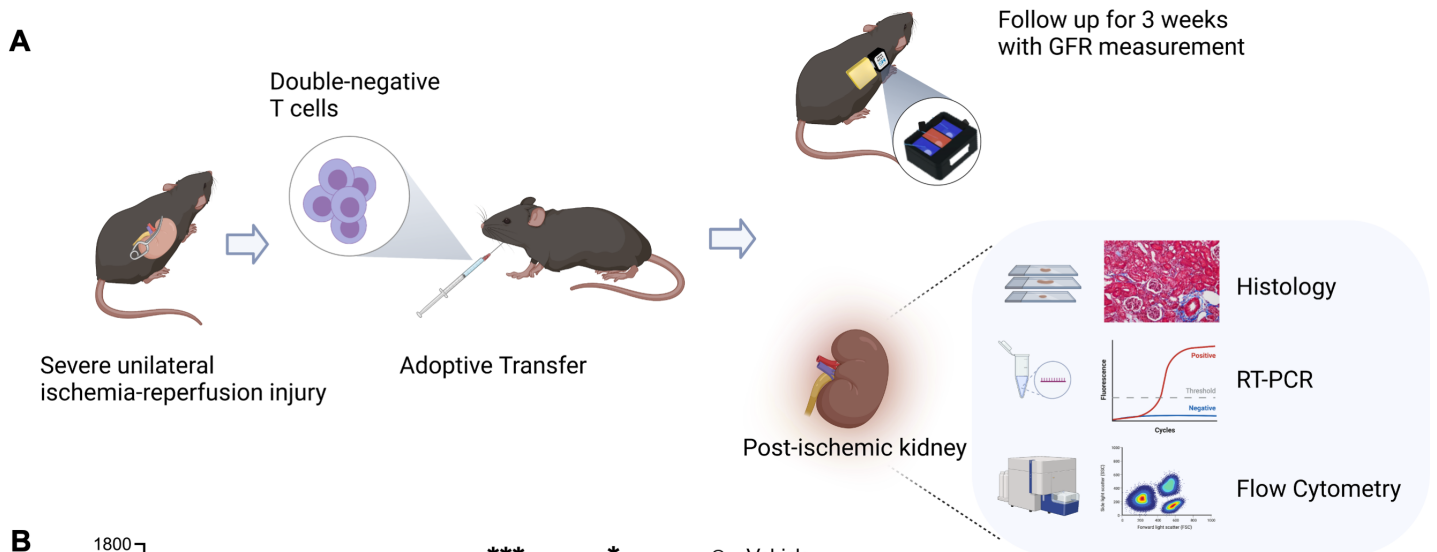


**Figure 8**

